LOW COMPLEXITY EQUALIZATION FOR OFDM IN DOUBLY SELECTIVE CHANNELS

A THESIS

SUBMITTED TO THE DEPARTMENT OF ELECTRICAL AND

ELECTRONICS ENGINEERING

AND THE INSTITUTE OF ENGINEERING AND SCIENCES

OF BILKENT UNIVERSITY

IN PARTIAL FULFILLMENT OF THE REQUIREMENTS

FOR THE DEGREE OF

MASTER OF SCIENCE

By

Alptekin PAMUK

May 2009

I certify that I have read this thesis and that in my opinion it is fully adequate, in scope and in quality, as a thesis for the degree of Master of Science.

Prof. Dr. Erdal ARIKAN(Supervisor)

I certify that I have read this thesis and that in my opinion it is fully adequate, in scope and in quality, as a thesis for the degree of Master of Science.

Assist. Prof. Dr. Defne AKTAŞ

I certify that I have read this thesis and that in my opinion it is fully adequate, in scope and in quality, as a thesis for the degree of Master of Science.

Assist. Prof. Dr. Sinan GEZİCİ

I certify that I have read this thesis and that in my opinion it is fully adequate, in scope and in quality, as a thesis for the degree of Master of Science.

Assist. Prof. Dr. Ali Özgür YILMAZ

Approved for the Institute of Engineering and Sciences:

Prof. Dr. Mehmet Baray
Director of Institute of Engineering and Sciences

ABSTRACT

LOW COMPLEXITY EQUALIZATION FOR OFDM IN DOUBLY SELECTIVE CHANNELS

Alptekin PAMUK
M.S. in Electrical and Electronics Engineering
Supervisor: Prof. Dr. Erdal ARIKAN
May 2009

In current standards Orthogonal Frequency Division Multiplex -OFDM- is widely used for its high resistance to multi-path environments and high spectral efficiency. However since the transmission duration is longer, it is affected from time variations of the channel more than single carrier systems. Orthogonality of sub-carriers are lost within an OFDM symbol and intercarrier interference(ICI) occurs as a result of time variation of the channel. Channel estimation and equalization become problematic, because the classical structures like MMSE require very complex operations. This thesis studies the channel equalization problem, as separate from the channel estimation problem. The thesis assumes that the channel coefficients are perfectly known and focuses on the estimation of data transmitted on each OFDM carrier. First, a survey of existing algorithms on channel equalization is given and simulations are provided to compare them in terms of complexity and performance under an OFDM system scenario that is consistent with the present WiMAX system parameters and operating conditions. As a novel contribution, the thesis proposes two new equalization methods by amending existing algorithms and shows that these modified algorithms improve the state-of-the-art in channel equalization in terms of complexity and

performance under certain high-mobility scenarios. Finally it is shown that the intercarrier interference cancellation problem remains a major impediment to the implementation of OFDM in high-mobility environments.

Keywords: OFDM, Equalization, Complexity, Performance Analysis, Time Varying, Intercarrier Interference

ÖZET

OFDM İÇİN FREKANS VE ZAMAN SEÇİÇİ KANALLARDA DÜŞÜK KARMAŞIKLI EŞLEME

Alptekin PAMUK
Elektrik ve Elektronik Mühendisliği Bölümü Yüksek Lisans
Tez Yöneticisi: Prof. Dr. Erdal ARIKAN
Mayıs 2009

Çok-yollu kanallardaki iyi performansı ve yüksek spektrum veriminden dolayı OFDM günümüz standartlarında yaygın olarak kullanılmaktadır. Ancak gönderme süresinin uzunluğundan dolayı tek taşıyıcılı sistemlere göre kanalın zamana göre değişiminden daha fazla etkilenmektedir. Bu durumda alt-taşıyıcıların birbiri arasındaki dikgenlik bozulmakta and taşıyıcılar arasında girişim oluşmaktadır. Kanal kestirimi ve sembol eşleme gittikçe problemli hale gelmektedir, çünkü klasik MMSE tipi yöntemler çok karmaşık işlemler gerektirmektedir. Bu tez kanal kestiriminin mükemmel olarak yapıldığını farz ederek sadece sembol eşleme problemiyle ilgilenmektedir. İlk olarak mevcut algoritmaların bir araştırması yapılmış ve bunlar WiMAX parametreleriyle benzer bir simülasyon ortamında test edilmiştir. Daha sonra mevcut algoritmalar modifiye edilerek iki yeni algoritma önerilmiş ve bu algoritmaların belli mobilite limitlerinde performans ve karmaşıklık açısından sembol kestiriminde optimum çözüme en yakın algoritmalar olduğu gösterilmiştir. Sonunda da alt-taşıyıcı girişiminin optimum olarak kaldırılamamasının yüksek mobiliteli kanallarda OFDM temelli sistemler kullanmanın önündeki en büyük engel olduğu gösterilmiştir.

Anahtar Kelimeler: OFDM, Eşleme, Karmaşıklık, Performans Analizi, Zamanla Değişen, Alt-taşıyıcı Girişimi

ACKNOWLEDGMENTS

I would like to thank my advisor Prof. Dr. Erdal ARIKAN for his guidance throughout my graduate education and my research. I would also like to thank Professors Sinan GEZİCİ, Defne AKTAŞ and Ali Özgür YILMAZ for serving as members of my committee.

Contents

List of Figures

List of Tables

To my dear wife who patiently supported me during my busy studies

LIST OF ABBREVIATIONS

OFDM	Orthogonal Frequency Division Multiplex
FFT	Fast Fourier Transform
FIR	Finite Impulse Response
ICI	Inter Carrier Interference
IFFT	Inverse Fast Fourier Transform
ISI	Inter Symbol Interference
LS	Least Squares
MF	Matched Filter
MMSE	Minimum Mean Square Error
SINR	Signal to Interference plus Noise Ratio
SISO	Single Input Single Output
SNR	Signal to Noise Ratio
SOS	Sum-of-sinosoids
TDL	Tapped Delay Line
WiMAX	Worldwide Interoperability for Microwave Access
WSSUS	Wide Sense Stationary Uncorrelated Scattering

Chapter 1

Introduction

Wireless systems have become very popular with the increase of the capacity of the integrated circuits, video broadcasting, telephone services, Internet services, etc. As time passed by a need for high data rates at high speeds has arisen. OFDM technique is widely used in current systems because of its superiority over single carrier systems at high data rates. On the other hand, with the increasing mobility, OFDM began to create problems. Complex processing is required to overcome the problems resulting from mobility. In this thesis we will look into that problem. The objectives of this thesis are

- to investigate the effects of time variation of the channel on OFDM
- to present the solutions proposed until now
- to propose new solutions
- to provide intuition for further developments

This chapter is organized as follows. The channel model is described at first. After that an introduction to OFDM will be made. System model used in the thesis will follow that. Then the target problem will be explained. Finally, an

outline of the thesis will be given. The notation used throughout the thesis is given below.

Notation: Upper-case(lower-case) bold face letters are used to denote matrices (column vectors). $(\cdot)^T$ and $(\cdot)^H$ represent transpose and complex conjugate transpose. We use the symbol $.*$ to denote element-wise product and $./$ to denote element-wise division. $|\cdot|$ indicates the absolute value. $E(\cdot)$ stands for the statistical expectation. $\Delta(\mathbf{A})$ is a vector consisting of the diagonal of $\mathbf{A}$. $\mathbf{I}_N$ denotes the N-by-N identity matrix, $\mathbf{0}_N$ denotes the N-by-1 zero vector and $\mathbf{F}$ denotes the unitary DFT matrix. $\mathbf{A}(m,n)$ indicates the entry in the m^{th} row and n^{th} column of $\mathbf{A}$. $\mathbf{A}(:,n)$ ($\mathbf{A}(n,:)$) is the n^{th} column (row) of $\mathbf{A}$. Finally, $\mathbf{A}(\mathbf{p},n)$ denotes elements in the n^{th} column whose row indexes are determined by the elements of the vector $\mathbf{p}$.

1.1 Wireless Channel Characteristics

There are different types of wireless channels depending on the application. The channel models for space applications, underwater applications, broadcasting applications, etc. are not the same. A drawing of the channel that we are dealing with is given in Figure 1.1[1]. The transmitted signal often does not directly reach to the receiver. Many reflected copies of the original signal are received instead. The delays, phases and powers of each reflected copy are random. The effects of that model may be listed as:

- *Inter-Symbol Interference(ISI):* (Considering single carrier systems) In time domain the symbol which is transmitted at time t_1 overlaps with another symbol which is sent at t_2. This event is called ISI. The receiver has to

[1]Picture is taken from http://ecee.colorado.edu/ liue/picture/graph/multipath.jpg

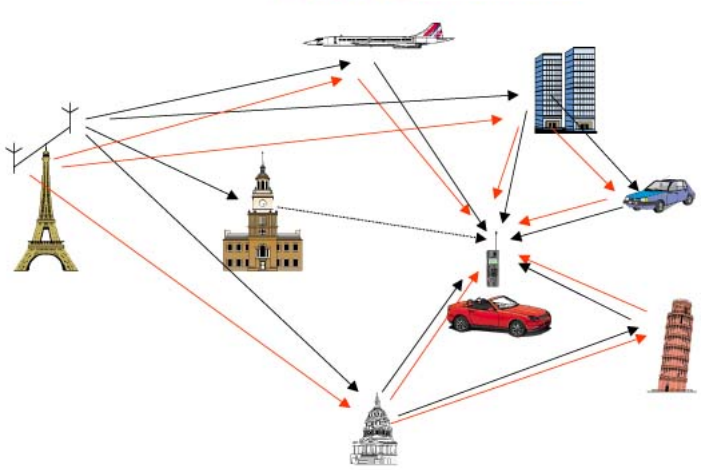

Figure 1.1: Multi-path Environment

somehow combine the received copies coherently which is not very simple, because delays, amplitudes and phases of the copies change in time.

- *Frequency Selectivity:* This is the result of *ISI* in frequency domain. The channel can be viewed as a natural FIR filter. Of course its frequency response is not expected to be flat because of the randomness. If the transmitted signal has a larger bandwidth than the coherence bandwidth of the channel (the bandwidth where the channel's frequency response can be considered as flat), the spectrum of the received signal is corrupted.

- *Fading:* Reflected copies have different phases, so they may sum up destructively at the receiver antenna. That part of the signal may be lost completely. This phenomenon is called in the literature as small scale fading.

- *Time Selectivity:* Since the receiver or transmitter moves, the amplitudes, phases and delays of all copies change in time. In other words channel's response changes in time, so the transmitted signal is treated differently in different time spans. For that reason *Time Selectivity* is viewed as the dual of *Frequency Selectivity*.

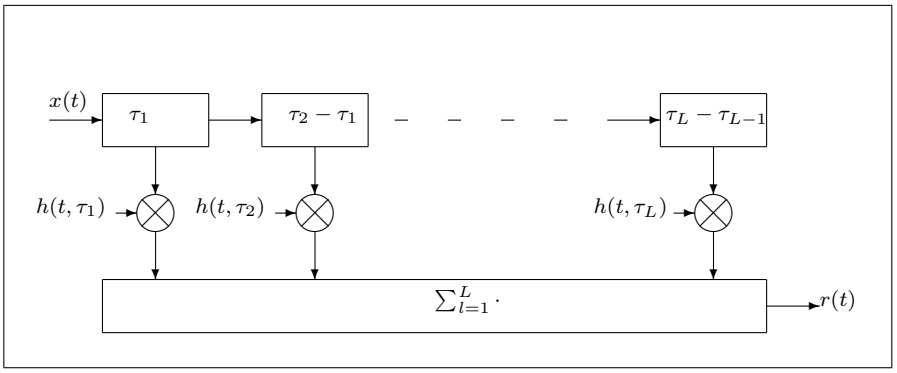

Figure 1.2: Variable spaced TDL Model

- *Doppler Spread:* The time selectivity of the channel creates an effect called Doppler Spread. The spectrum of the transmitted signal is shifted and squeezed (or broadened) when it reaches to the receiver. Only time selectivity is enough for this effect, multi-path environment is not necessary.

In the literature many papers are published regarding the modeling of time and frequency selective channels. The reader can find a good overview of the suggested models and references in [1]. Time and frequency selectivity are mutually related. However as many authors did, we will assume WSSUS model [2] so that we can model these two selectivities independently for practical issues.

Let $h(t, \tau_l)$ be the response of the l^{th} path at time t whose delay is τ_l. As stated above, this channel can be viewed as an analog filter like in Figure 1.2 ([3]). By looking at the figure output can be expressed as $r(t) = \sum_{l=1}^{L} h(t, \tau_l)x(\tau - \tau_l)$ where L is the total number of paths. However it is not easy to use this model, because there may be a large number of paths and the delay of each path will most likely not be an integer multiple of the system's sampling frequency $f_s = T_s^{-1}$. A more useful model is using taps which are equally spaced in time([1]). This model is pictured in Figure 1.3. Each tap is separated by a time difference equal to sampling interval of the system, coefficients are again time-varying. The relation between $h(t, \tau_l)$ and $g_i(t)$ can be found in [1].

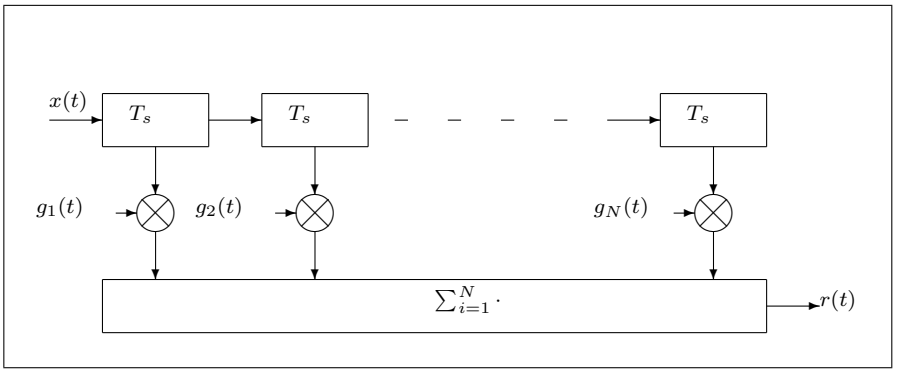

Figure 1.3: Equally spaced TDL Model

For the complex coefficients and delays in Figure 1.2 exponential power delay profile is used in the literature. However in this thesis we used ITU's models which will be given later. With this model we complete the frequency selectivity modeling. For the time selectivity, we have to choose a statistical behavior for time varying complex coefficients. Based on WSSUS assumption the auto-correlation function of $h(t, \tau_l)$'s is given as

$$E\left[h(t_1, \tau_{l_1}) h^*(t_2, \tau_{l_2})\right] = R_h(t_2 - t_1, \tau_{l_1}) \delta(\tau_{l_2} - \tau_{l_1}) \tag{1.1}$$

where $\delta(\cdot)$ is the Dirac's delta function. As stated earlier the autocorrelation function is separable in time and delay [4] because of WSSUS assumption.

$$R_h(t_2 - t_1, \tau_{l_1}) = \kappa_t(t_2 - t_1) \kappa_l(\tau_{l_1}) \tag{1.2}$$

where $\kappa_l(\tau_{l_1})$ is the multi-path intensity profile (defines the average power on l^{th} path given in Figure 1.2) and $\kappa_t(t_2 - t_1)$ is time correlation function (defines the time varying behavior of each tap coefficient). The Fourier transform of $\kappa_t(t_2 - t_1)$ is called Doppler power spectrum $\kappa_t(f)$. There are different spectrum models, but we will use the classical time correlation function based on Jakes' model that is $\kappa_t(t_2 - t_1) = J_0(2\pi(t_2 - t_1) f_d)$ where $J_0(\cdot)$ is the zeroth order Bessel function of the first kind and f_d is the maximum Doppler shift in the system. There are various ways to simulate parameters having this statistical characteristics. We used the sum-of-sinosoids(SOS) model of [5].

1.2 OFDM Technology

The first OFDM structure was presented by Chang in 1966 [6]. Differently from current systems, a group of sinusoidal generators were used. In 1971 using DFT for transmission is proposed by [7]. The first modern OFDM was born then. After that *Cyclic Prefix OFDM* became indispensable and widely used for *Inter Block Interference* combating in multi-path channels. To mitigate channel nulls in the frequency domain *Coded OFDM* is given in [8] at the expense of bandwidth over-expansion. More recently another modification is proposed, *Zero Padding OFDM*(*ZP-OFDM*) [9]. Its advantages are better linearity, compensation of channel nulls and same bandwidth characteristics with *Cyclic Prefix OFDM*. On the other hand the complexity of the receiver increases.

By the nature of OFDM technique, the frequency selective channels become flat channels. OFDM is widely used in the recent wireless standards because of that. For example; in the eight release of 3GPP project, in the digital video broadcasting standards DVB-S, DVB-S2, DVH-H and DVB-T, in wireless network standards 802.11a to 802.16e (an introduction can be found in [10]), in high speed wire-line transmissions like ADSL [11], etc.

We will give a brief description of *Cyclic Prefix OFDM*. Detailed information can be obtained from [12]. Serially incoming bits from an information source are first converted to a parallel block and modulated by conventional methods like PSK or QAM modulation. Denote the modulated vector by $\mathbf{s}$ whose size is N by 1. Then IFFT operation is performed over $\mathbf{s}$:

$$\mathbf{x} = \mathbf{F}_N^H \mathbf{s} \tag{1.3}$$

In time domain a portion from the end of $\mathbf{x}$ is added to the beginning of that vector.

$$\mathbf{x}_{CP} = [\mathbf{x}(c:N)^T \quad \mathbf{x}^T]^T \tag{1.4}$$

where c is a design parameter. This operation is called *Cyclic Prefix Insertion*. Assuming a flat channel with unit power, the receiver first removes the cyclic prefix. Then N-point FFT operation is performed. The obtained symbol vector is demodulated and converted to a serial bit-stream.

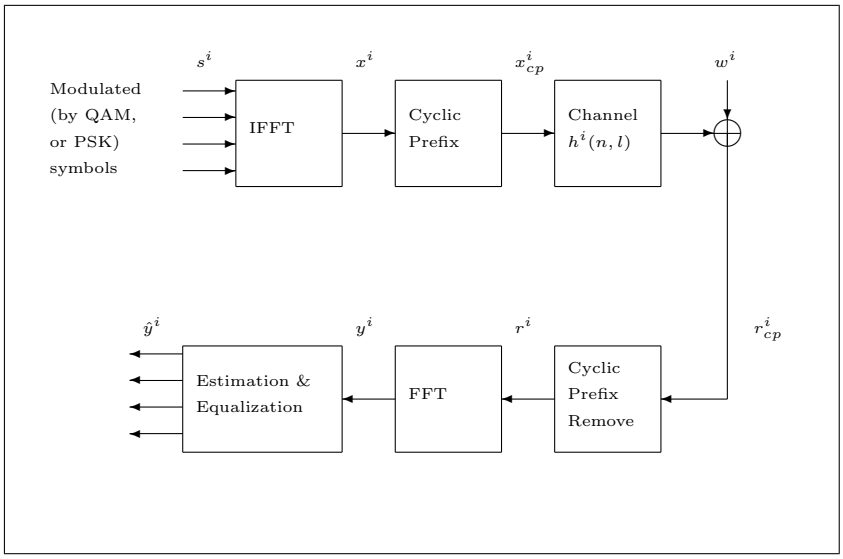

Figure 1.4: System Model

1.3 System Model

In this section we will describe our baseband system model which is illustrated in Figure 1.4. During the i^{th} OFDM symbol period, P-modulated frequency domain symbols $\mathbf{s}^i = [\mathbf{s}^i(0) \ \ldots \ \mathbf{s}^i(0)]^T$ are collected and converted to time domain signal by IFFT operation

$$x^i(n) = \frac{1}{\sqrt{N}} \sum_{k=0}^{P-1} \mathbf{s}^i(k) e^{j2\pi kn/N} \tag{1.5}$$

where N and P are the total number of sub-carriers and the number of active sub-carriers respectively. Normally $P < N$ because some of the sub-carriers are not modulated and left for guard band. However for simplicity of notation we will take $P = N$. After IFFT, a portion from the end of $\mathbf{x}$ is added to the beginning of the time domain vector.

$$\mathbf{x}_{CP} = [\mathbf{x}(c:N)^T \ \ \mathbf{x}^T]^T \tag{1.6}$$

where c is a design parameter and should be chosen bigger than the inverse of coherence bandwidth of the channel to get rid of ISI. Then $\mathbf{x}_{CP}$ is sent through the time varying noisy channel. We assume perfect timing and frequency synchronization is performed. The received signal after removing cyclic prefix is

expressed as:

$$r^i(n) = \sum_{l=0}^{L-1} h^i(n,l)x^i(n-l) + w^i(n) \tag{1.7}$$

where $h^i(n,l) \stackrel{def}{=} h(iN + i(N-c+1) + n, l)$ is the response of l^{th} path of the channel at time n, L is the total number of paths and $w^i(n)$ is the white noise. Defining $H^i(k,n) = \sum_{l=0}^{L-1} h^i(n,l)\exp(-j2\pi lk/N)$, i.e. the frequency response of the channel at time n, the received signal can be expressed as:

$$r^i(n) = \frac{1}{\sqrt{N}} \sum_{k=0}^{N-1} \mathbf{s}_k^i H^i(k,n) e^{j2\pi kn/N} + w^i(n) \tag{1.8}$$

As it is seen the channel introduces a complex and time varying multiplier to each sub-carrier. Some receiver structures use the above time domain signal for equalization [13]. However we will use the frequency domain signal. Performing FFT on r^i gives:

$$\mathbf{y}^i(k) = \frac{1}{\sqrt{N}} \sum_{k=0}^{N-1} r^i(n) e^{-j2\pi kn/N} \tag{1.9}$$

Alternatively it can be expressed with its most famous form in the literature

$$\begin{aligned}
&\mathbf{y}^i(k) = \mathbf{s}^i(k)\mathbf{A}^i(k,k) + \mathbf{ICI}^i(k) + \mathbf{w}^i(k) \\
&\mathbf{A}^i(k,k) = \tfrac{1}{N}\textstyle\sum_{n=0}^{N-1} \mathbf{H}^i(k,n) \\
&\mathbf{ICI}^i(k) = \tfrac{1}{N}\textstyle\sum_{m=0,m\neq k}^{P-1} \mathbf{s}^i(m) \sum_{n=0}^{N-1} \mathbf{H}^i(m,n) e^{j2\pi(m-k)n/N} \\
&\mathbf{w}^i(k) = \tfrac{1}{\sqrt{N}}\textstyle\sum_{k=0}^{N-1} w^i(n) e^{-j2\pi kn/N}
\end{aligned} \tag{1.10}$$

The $ICI^i(k)$'s represent the inter-carrier interference which is caused by the time varying nature of the channel. One can observe that if the channel is not time varying $ICI^i(k) = 0$ since $\mathbf{H}^i$ will not depend on time index n and up to some mobilities this interference can be neglected [14]. We also want to note that $\mathbf{A}^i(k,k)$'s are not equal if there are more than one resolvable paths, i.e, if it is a frequency selective channel. The equations in (1.10) can be expressed in matrix

notation as

$$\begin{aligned} \mathbf{y}^i &= \mathbf{A}^i\mathbf{s}^i + \mathbf{w}^i \\ \mathbf{y}^i &= [\mathbf{y}^i(0) \ \ldots \ \mathbf{y}^i(N-1)]^T \\ \mathbf{s}^i &= [\mathbf{s}^i(0) \ \ldots \ \mathbf{s}^i(N-1)]^T \\ \mathbf{A}^i(k,m) &= \tfrac{1}{N}\textstyle\sum_{n=0}^{N-1} \mathbf{H}^i(m,n)e^{j2\pi(m-k)n/N} \\ \mathbf{w}^i &= [\mathbf{w}^i(0) \ \ldots \ \mathbf{w}^i(N-1)]^T \end{aligned} \tag{1.11}$$

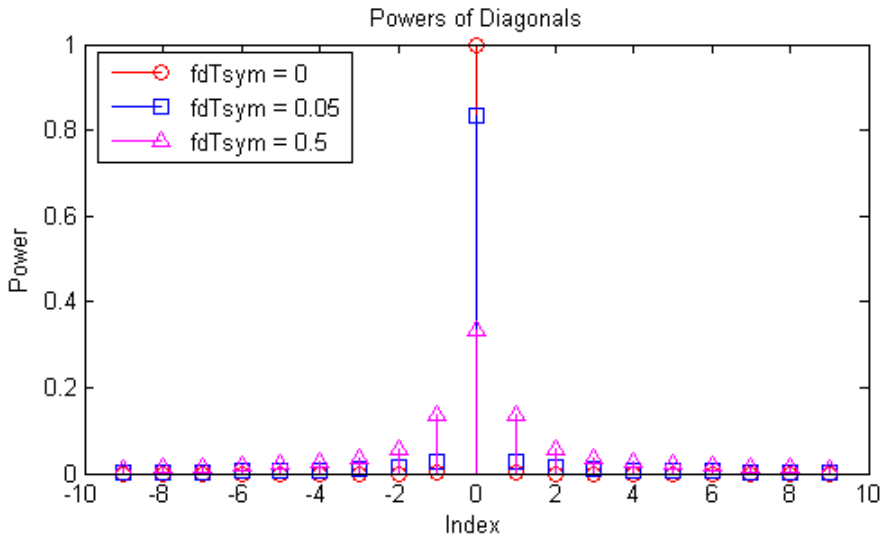

Figure 1.5: Powers of diagonals

The superscript i will be dropped for simplicity in the remaining parts of the thesis. ICI is a very important phenomenon in OFDM, thus it will be explained in detail. The channel matrix $\mathbf{A}$ given in Eq. (1.11) is a diagonal matrix if the channel is stationary during the transmission period. Thus the receiver can simply divide the observation vector by the diagonal of the channel matrix (one tap equalizer). However as the time variation (or mobility) of the channel increases -which is measured by $f_D T_{SYM}$ where f_D is the maximum Doppler frequency in the system and T_{SYM} is the OFDM symbol duration- the matrix is no longer diagonal. Fortunately it has a banded structure in that case which is shown in Figure 1.6. The average powers of the main diagonal, super-diagonals and sub-diagonals are given in Figure 1.5. The one in the center is the power of the main diagonal, the one on the right is the power of the first super-diagonal

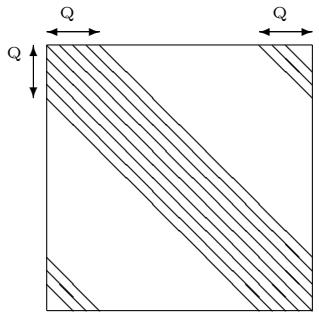

Figure 1.6: Banded structure of channel matrix

and the one on the left is the power of the first sub-diagonal, the next ones belong to second super and sub diagonals and so on. The spread of energy is clearly seen from that figure. To describe ICI mathematically, assume only one sub-carrier is modulated at the transmitter, the rest is left as zero. By using the Eq.(1.11), the observation vector at the receiver can be expressed as

$$\mathbf{y} = \mathbf{A}(:, K)\mathbf{s}(K) + \mathbf{w} \tag{1.12}$$

where K is the index of modulated sub-carrier. Eq. (1.12) suggests that time varying channel provides a frequency diversity. Not all elements in $\mathbf{A}(:, K)$ are significant, so the insignificant elements can be disregarded for practical issues. So we are left with a banded vector whose bandwidth depends on $f_D T_{SYM}$. Let this bandwidth be Q diagonals and define $\mathbf{p} = [K - Q \ \ldots \ K \ \ldots \ K + Q]$ (summations are in modulo-N). We can rewrite Eq.(1.12) as

$$\mathbf{y(p)} = \mathbf{A}(\mathbf{p}, K)\mathbf{s}(K) + \mathbf{w}(\mathbf{p}) \tag{1.13}$$

In other words the effect of the symbol at K^{th} sub-carrier can be seen at Q neighboring sub-carriers providing a natural frequency diversity. However a problem arises when all the sub-carriers are modulated, because the observation element at the K^{th} index will then be a linear combination of $2Q + 1$ symbols plus white noise. To benefit from diversity, this interference coming neighboring symbols should be removed first which is not an easy task.

1.4 Problem Description and State-of-The-Art Solution

The problems of OFDM technoque can be listed as:

- Timing Synchronization
- Frequency Synchronization
- Peak to Average Power Ratio
- CSI(or Channel) Estimation
- Symbol Estimation (or Equalization)

We suggest the books [12], [15], [16] and [17] for further discussions of the first three and continue with the remaining two problems. As the name implies *CSI estimation* is extracting channel matrix $\mathbf{A}$ in Eq.(1.11). However at high mobilities and in multi-path environment there exists $N(2Q+1)$ unknowns to be estimated. But there are at most N equations even though the receiver knows all transmitted symbols, so channel estimation becomes really difficult. *Symbol estimation* (or *equalization*) is estimating the transmitted symbol vector from the observation vector given the channel estimation. Channel estimation and equalization can be done jointly and iteratively, i.e., first channel parameters are estimated, then an equalization performed, after that a second channel estimation can be done using the symbol estimates and a second equalization using the new channel parameters and so on. In this thesis we will only focus on the *equalization* problem and assume that a perfect channel estimation is available.

After defining the target problem, the solution is in fact obvious. One can simply invert the channel matrix that is :

$$\hat{\mathbf{s}} = \mathbf{A}^{-1}\mathbf{y} = \mathbf{s} + \mathbf{A}^{-1}\mathbf{w} \tag{1.14}$$

which is a simple solution. However there is another problem in this case; complexity. The complexity of matrix inversion is in the order of N^3. N is at least 512 in current standards, so $512 * 512 * 512$ is far from being realizable with current technology. Based on this fact, the state-of-the-art solution is defined in this thesis as the one that

- reaches the performance of *PB2* which will be defined in the next chapter
- has a complexity less than or equal to $N \log N$ (which is the complexity of FFT algorithm)

1.5 Contributions of the Thesis

The equalization and channel estimation problems are considered jointly in most of the papers. There are not many papers which only focus on equalization. We collected many of the proposed equalizers and two methods which enhance the performance of the equalizer, simulated them with real world scenarios and compared the performances.

We performed simulations to show the properties that a good equalizer must have. Then we provided intuitions to obtain or at least to get close to a state-of-the-art algorithm.

We proposed two modifications to equalizers given in other papers. With the first modification, the new equalizer got very close to state-of-the-art definition, but only up to some mobilities. The second modification was proposed to an equalizer which was the best of all at high mobilities. With our modification the complexity was reduced and the performance did not change.

1.6 Outline

In the second chapter we will first give a definition of simulation parameters. Then the simulated equalizers will be presented in detail. Some simulations will be done regarding the effect of mobility on OFDM. After that the performances and complexities of the presented equalizers will be compared. At the end we will give a summary of what is done and comment on the results obtained.

In the third chapter the two proposed modifications will be explained. Following that the simulations will be done with real world scenarios. Their performances will be compared with the best of the algorithms given in chapter two. Again a complexity comparison will be done. Finally some of the equalizers will be suggested for use in real world systems.

In the fourth and the last chapter a summary of the thesis and the results will be given. Then future work will be explained.

Chapter 2

Algorithms In The Literature

In this chapter the simulation scenarios will be introduced at first. Next, the existing solutions for equalization will be presented. After that simulations will be done and finally the results will be interpreted.

2.1 Simulation Scenarios

Recall the system model given in Chapter 1. The equations describing the system model were:

$$\begin{aligned} \mathbf{y}^i(k) &= \tfrac{1}{\sqrt{N}} \textstyle\sum_{k=0}^{N-1} r^i(n) e^{-j2\pi kn/N} \\ \mathbf{y} &= \mathbf{As} + \mathbf{w} \end{aligned} \tag{2.1}$$

OFDM system parameters that were given in [18] are taken as the basis for our study. Our modified parameters are given in Table 2.1.

We have given the channel model in the first chapter. Recall Eq. (1.2), continuous time domain expression was given there for $\kappa_t(t_2 - t_1)$. Since we will work in discrete domain, we have to sample it with $f_s = T_s^{-1}$:

$$\kappa_n(n_2 - n_1) = \kappa_t(n_2 T_s - n_1 T_s) = J_0(2\pi(n_2 - n_1) f_d / f_s) \tag{2.2}$$

Parameter	Description	Value
f_c	Carrier Frequency	2.5 GHz
BW	Total bandwidth	2.5 MHz
N_{FFT}	No. of points in full FFT	256
f_s	Sampling frequency	2.8 MHz
Δ_f	Subcarrier spacing	10.9375 kHz
$T_{SYM} = 1/\Delta_f$	Symbol duration without cyclic prefix	91.43 us
CP	Cyclic prefix length (fraction of T_0)	1/8
N_G	No of guard band carriers (fraction of N_{FFT})	1/8
N_f	No of OFDM Symbols in a Frame	50
ν_D	Doppler Speed	0km/h to 2360km/h

Table 2.1: Simulation Parameters

We used the SOS method of [3] to synthesize the coefficients having this statistics. For the multi-path intensity profile $\kappa_l(\tau_l)$, we used ITU's 'Modified Vehicular Channel A' parameters given in [18]. Those parameters are written in Table 2.2. To model the channel with these parameters as in Figure 1.3, we used the method in [1]. As stated previously we will assume that the channel state information is perfectly available.

Path Index	Modified Pedestrian B		Modified Vehicular A	
	Power (dB)	Delay (ns)	Power (dB)	Delay (ns)
1	-1.175	0	-3.1031	0
2	0	40	-0.4166	50
3	-0.1729	70	0	90
4	-0.2113	120	-1.0065	130
5	-0.2661	210	-1.4083	270
6	-0.3963	250	-1.4436	300
7	-4.32	290	-1.5443	390
8	-1.1608	350	-4.0437	420
9	-10.4232	780	-16.6369	670
10	-5.7198	830	-14.3955	750

11	-3.4798	880	-4.9259	770
12	-4.1745	920	-16.516	800
13	-10.1101	1200	-9.2222	1040
14	-5.646	1250	-11.9058	1060
15	-10.0817	1310	-10.1378	1070
16	-9.4109	1350	-14.1861	1190
17	-13.9434	2290	-16.9901	1670
18	-9.1845	2350	-13.2515	1710
19	-5.5766	2380	-14.8881	1820
20	-7.6455	2400	-30.348	1840
21	-38.1923	3700	-19.5257	2480
22	-22.3097	3730	-19.0286	2500
23	-26.0472	3760	-38.1504	2540
24	-21.6155	3870	-20.7436	2620

Table 2.2: ITU Power Delay Profiles

The pedestrian profiles are used in low mobility cases while the vehicular are used in high mobility cases which is given as 120km/h at most in Table 3 in [18]. We also simulated unrealistic speeds in our simulations. Because as stated previously the rate of change of channel is measured by $f_d T_{SYM}$, not just by the speed. In other words the time variation corresponding to a speed of 1000km/h with our parameters may occur with lower speeds in another system.

The following scenarios will be simulated with the given parameters above:

- The effect of energy spreading in time varying channels
- The performance comparison of equalizers under different channel conditions

- The effect of performance enhancement methods
- Complexity comparison of some of the simulated equalizers.

2.2 Description of the Simulated Algorithm(s)

The equalization algorithms that will be presented in this section can be divided into four groups; high complexity block, low complexity block, high complexity serial and low complexity serial. The term 'complexity' is obvious. The block equalizers estimate all the symbols in one shot. For example the one in Eq. (1.14) was a block equalizer. In serial equalization at first a symbol is estimated, then the interference (remember equations (1.12) and (1.13)) resulting from that symbol is removed from the observation vector. After that the next symbol is estimated and its interference is removed and so on. Based on this classification the existing solutions can be listed as:

- ☞ high complexity block
  - Classical MF, MMSE and LS methods as described in [13] (in short MF, MMSE, LS).
- ☞ low complexity block
  - Equalization by LDL decomposition of [19] (in short LDL).
  - Block decision feedback equalization of [20] (in short BDFE).
  - Block Turbo Iterative equalizer of [21] (in short TB).
- ☞ high complexity serial
  - Serial MMSE equalizer of [22] (in short CAI).
- ☞ low complexity serial
  - Serial Turbo Iterative equalizer of [14] (in short TI).

Also we need a benchmark to compare those algorithms. We presented two benchmarks in this section (in short PB1, PB2). Finally, we implemented two performance enhancement methods. These are

- Time domain windowing given in [20] and [14].
- Parallel interference cancellation given in [22].

Before going into details of the algorithms it will be useful to introduce a parameter; Q. It will be used in most of the descriptions below. It is a measure of bandwidth assumption (like the one in Eq. (1.13)), and is selected by $\lceil f_d T_{SYM} \rceil + 1$ as suggested in [14], where $\lceil x \rceil$ is the ceiling operation(It was mostly 2 in our simulations).

PB1 and PB2: We have to compare simulated equalizers with a performance bound. A method to simulate a bound is given in [22]. Only one sub-carrier is modulated in an OFDM symbol and matched filter type equalizer is used at the receiver that is

$$\hat{\mathbf{s}}(k) = \mathbf{a}^H \mathbf{y} / (\mathbf{a}^H \mathbf{a}) \tag{2.3}$$

where k is the index of the modulated sub-carrier and $\mathbf{a} = \mathbf{A}(:, k)$. This is not a band-limited equalizer, i.e. using the whole observation vector. The low complexity equalizers in this section make a bandwidth assumption, so we modified the structure given in Eq. (2.3). We used a band-limited version and named it *PB2*.

$$\hat{\mathbf{s}}(k) = \mathbf{a}_k^H \mathbf{y}_k / (\mathbf{a}_k^H \mathbf{a}_k) \tag{2.4}$$

where $\mathbf{a}_k = \mathbf{A}(k - Q : k + Q, k)$ and $\mathbf{y}_k = \mathbf{y}(k - Q : k + Q)$. So *PB2* uses only $2Q + 1$ observation elements. To show the importance of energy spreading in time varying channels we simulated another bound, *PB1*. *PB1* uses only the observation element that the transmitter modulated

$$\hat{\mathbf{s}}(k) = \mathbf{A}^H(k, k)\mathbf{y}(k) / \left|\mathbf{A}(k, k)\right|^2 \tag{2.5}$$

MF, LS and MMSE: In [13], where those equalizers are given, the equalization is performed in time domain. However we made equalization in frequency domain with the same equations. The *MF* equalizer is a classic matched-filter

$$\hat{\mathbf{s}} = (\mathbf{A}^H \mathbf{y})./\Delta(\mathbf{A}^H \mathbf{A}) \tag{2.6}$$

This equalizer works best if $\mathbf{A}^H \mathbf{A}$ is a diagonal matrix, i.e., if the channel is not or almost stationary during the transmission of OFDM symbol. Recall Eq. (1.11) here. The linear structure leads to classical least square problem [23]. The *LS* equalizer is given by

$$\hat{\mathbf{s}} = (\mathbf{A}^H \mathbf{A})^{-1} \mathbf{A}^H \mathbf{y} \tag{2.7}$$

The simulation results for *MF* and *LS* are not given because of their poor performance and to reduce the complexity in the graphics. The last equalizer given in [13] is *MMSE*. It is given by

$$\hat{\mathbf{s}} = (\mathbf{A}^H \mathbf{A} + \sigma^2 I_N)^{-1} \mathbf{A}^H \mathbf{y} \tag{2.8}$$

where σ^2 is the inverse of SNR.

CAI: The algorithm proposed by [22] serially equalizes the symbols. In the previous section *CAI* was presented as a non-banded equalizer, actually it is not. At the ICI cancellation stage all the symbols are used, however at the equalization stage only $2Q+1$ observation elements are used. It can be classified as half-banded equalizer because of that.

For each sub-carrier, a sub-matrix is extracted from the channel matrix and MMSE equalization is performed. Then interference to the other sub-carriers are removed from the observation vector. The sub-carrier with the best received power is selected as the starting point. This is done by ordering the norm of the columns of the channel matrix. Let k^{th} sub-carrier has the highest power and define $\rho_k = [k-Q \ \ldots \ k \ \ldots \ k+Q]$ and $\mathbf{m}_k = (\mathbf{A}(\rho_k, :)\mathbf{A}^H(\rho_k, :$

$) + \sigma^2 I_{2Q+1})^{-1}\mathbf{A}(\rho_k, k)$. In the equalization stage

$$\hat{\mathbf{s}}(k) = \mathbf{m}_k^H \mathbf{y}(\rho_k) \tag{2.9}$$

is performed and in the interference removing stage the following operation is done

$$\mathbf{y} = \mathbf{y} - \mathbf{A}(:, k)\hat{\mathbf{s}}(k) \tag{2.10}$$

After completing the equalization of the whole sub-carriers, another iteration could be started. But we did not do that, yet its performance was still very good.

LDL: In [19] the *MMSE* equalizer is put into a banded form. The matrix inversion in that structure is done by LDL^H factorization. At the first step the channel matrix is multiplied by a Toeplitz matrix T, $\mathbf{B} = \mathbf{T}. * \mathbf{A}$. The elements of the matrix $\mathbf{T}$ are all zero except the main diagonal, Q sub-diagonals and Q super-diagonals (which are one). If we rewrite the equation for *MMSE* algorithm with this new banded channel matrix, we get

$$\hat{\mathbf{s}} = (\mathbf{B}^H\mathbf{B} + \sigma^2 I_N)^{-1}\mathbf{B}^H\mathbf{y} \tag{2.11}$$

Since $\mathbf{M} = (\mathbf{B}^H\mathbf{B} + \sigma^2 I_N)$ is a banded matrix with lower and upper bandwidth $2Q$, it can be decomposed by LDL^H factorization. Then the inversion is performed by band forward and backward substitution. The pseudo code for the factorization is given in Figure 2.1

BDFE: A block decision feedback equalizer is given in [20]. The structure of BDFE is given in Figure 2.2. The feed-forward filter F_f and the feedback filter F_B are designed based on the MMSE approach of [24]. Like *LDL*, define $\mathbf{M} = (\mathbf{B}^H\mathbf{B} + \sigma^2 I_N)$ where channel matrix $\mathbf{B}$ is $\mathbf{A}. * \mathbf{T}$. Again $\mathbf{M}$ is factorized as given in Figure 2.1. After that, the filters can be expressed as:

$$\mathbf{F}_B = \mathbf{L}^H - \mathbf{I}_N \tag{2.12}$$

$\mathbf{L} = \mathbf{I}_N; \mathbf{D} = \mathbf{M}. * I_N; \mathbf{v} = \mathbf{0}_{Nx1};$
$for\ j = 1 : N$
$\quad m = max\{1, j - 2Q\}; M = min\{j + 2Q, N\};$
$\quad for\ i = m : j - 1$
$\quad\quad \mathbf{v}(i) = \mathbf{L}^*(j,i)\mathbf{D}(i,i);$
$\quad end$
$\quad \mathbf{v}(j) = \mathbf{M}(j,j) - \mathbf{L}(j, m : j-1)\mathbf{v}(m : j-1);$
$\quad \mathbf{D}(j,j) = \mathbf{v}(j);$
$\quad \mathbf{L}(j+1 : M, j) = \frac{\mathbf{M}(j+1:M,j) - \mathbf{L}(j+1:M, m:j-1)\mathbf{v}(m:j-1)}{\mathbf{v}(j)}$
end

Figure 2.1: The pseudo code for LDL^H factorization

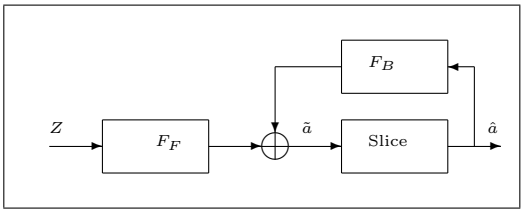

Figure 2.2: The structure of BDFE Equalizer

$$\mathbf{F}_F = \mathbf{D}^{-1}\mathbf{L}^{-1}\mathbf{B}^H \tag{2.13}$$

In the simulations the algorithm was iterated 5 times.

TI: A new turbo approach is suggested in [14]. In fact four types of methods are described in that paper, however we have selected the serial iterative equalizer which is also as good as the other methods. Other methods use the LLR info, while the one that we chose does not. The equalizer is

$$\mathbf{f}_k = (\mathbf{A}_k\mathbf{A}_k^H + \sigma^2 I_{2Q+1})^{-1}\mathbf{a}_k \tag{2.14}$$

$$\hat{\mathbf{s}}(k) = \bar{\mathbf{s}}(k) + \mathbf{f}_k^H(\mathbf{Y}(k - Q : k + Q) - \mathbf{A}_k\bar{\mathbf{s}}(k - 2Q : k + 2Q)) \tag{2.15}$$

where $\mathbf{A}_k = \mathbf{A}(k-Q : k+Q, k-2Q : k+2Q)$, $\mathbf{a}_k = \mathbf{A}(k-Q : k+Q, k)$ and $\bar{\mathbf{s}}(k)$ is obtained by making hard-decision on $\hat{\mathbf{s}}(k)$. At the beginning of equalization process, $\bar{\mathbf{s}}$ is initialized to $\mathbf{0}_N$.

TB: A block type equalizer is proposed based on turbo approach in [21]. The MMSE estimate of the OFDM symbol is given by

$$\hat{\mathbf{s}} = \mathbf{m} + \mathbf{G}^H(\mathbf{y} - \mathbf{B}\mathbf{m}) \tag{2.16}$$

$$\mathbf{G} = (\mathbf{B}\mathbf{V}\mathbf{B}^H + \sigma^2\mathbf{I}_N)^{-1}\mathbf{B}\mathbf{V} \tag{2.17}$$

where the channel matrix $\mathbf{B}$ is obtained by **A.*T** and $\mathbf{T}$ is a Toeplitz matrix as defined in *LDL*, $\mathbf{m}(i) = E(\hat{\mathbf{s}}(i))$ and $\mathbf{V}$ =diag($\mathbf{v}$), $\mathbf{v}$ =Cov($\hat{\mathbf{s}}(i), \hat{\mathbf{s}}(i)$). In the second step the LLR values are calculated. Using the new LLR values the vectors $\mathbf{m}$ and $\mathbf{v}$ are updated. In the simulations the algorithm was iterated 3 times.

WINDOWING: To squeeze ICI components into a few sub-carriers, some windows are developed in [20] and [14]. The one in [14] is obtained by defining a metric; SINR (signal to noise plus interference ratio). It is basically the ratio of the energy in the desired bandwidth(within Q neighboring sub-carriers) and the energy out of the band assuming windowing is performed. The resulting maximization coefficients of SINR are

$$\mathbf{w} = v(\mathbf{C}. * \mathbf{R}, (\sigma^2 + \sum_l \kappa_l^2(l))\mathbf{I}_N - \mathbf{C}. * \mathbf{R}) \tag{2.18}$$

where $v(\mathbf{B}, \mathbf{C})$ denotes the principle generalized eigenvalue of the matrix pair $(\mathbf{B}, \mathbf{C})$, $\mathbf{R}$ is the autocorrelation of the channel matrix whose elements are $\mathbf{R}(r, c) = \kappa_n(r-c)\sum_l \kappa_l^2(l)$ and $\mathbf{C}(r, c) = \sin(\frac{\pi}{N}(2Q+1)(r-c))/(N\sin(\frac{\pi}{N}(r-c)))$.

In [20] a similar method is applied by also adding another constraint. The window coefficients are obtained in this case by

$$\mathbf{w}_q = v(\tilde{\mathbf{F}}^H(\mathbf{C}. * \mathbf{R})\tilde{\mathbf{F}}) \tag{2.19}$$

$$\mathbf{w} = \tilde{\mathbf{F}}\mathbf{w}_q \tag{2.20}$$

where $\mathbf{C}$ and $\mathbf{R}$ are as defined before and $\tilde{\mathbf{F}} = [\mathbf{f}_{-Q}, \ldots, \mathbf{f}_0, \ldots, \mathbf{f}_Q]$, $\mathbf{f}_i$ is the i^th column of the FFT matrix.

After obtaining filters for a given channel, the windowing is performed in the time domain

$$\mathbf{r}_w = w. * \mathbf{r} \tag{2.21}$$

where $\mathbf{r}$ is the observation vector in the time domain. Windowing is a very low complexity operation and squeezes ICI very well.

PIC: Parallel interference cancellation is suggested as a performance improving method after equalizer in [22]. At first all ICI components are removed from the observation vector using the symbol estimates and symbol estimation is done like *PB2*.

$$\begin{aligned} \hat{\mathbf{y}}_k &= \mathbf{y}(\mathbf{p}_k) - \textstyle\sum_{m=0,m\neq k}^{N-1} \mathbf{A}(\mathbf{p}_k, m)\hat{\mathbf{s}}(m) \\ \hat{\mathbf{s}}_k &= \mathbf{A}(\mathbf{p}_k, k)^H \hat{\mathbf{y}}_k / (\mathbf{A}(\mathbf{p}_k, k)^H \mathbf{A}(\mathbf{p}_k, k)) \end{aligned} \tag{2.22}$$

where $\mathbf{p}_k = [k-Q \ \ldots \ k \ \ldots \ k+Q]$. *PIC* method works well, on the other hand its complexity is even more than some of the equalizers.

2.3 Simulation Results

The simulation parameters and scenarios were given in Section 2.1. In this section the simulation results will be given.

The effect of energy spreading in time varying channels: The simulations are shown in Figures 2.3-2.5.

- In Figure 2.3 it is seen that *PB2* outperforms *PB1* and the performance gap increases with the mobility. It was expected since *PB2* uses all the spread energy while *PB1* does not (see Figure 1.5).
- In Figure 2.4 it is seen that the effect of natural frequency diversity. Because of diversity *PB2* performs better at high mobilities.
- In Figure 2.5 it is seen that the PB1 performs a little better than PB2. It is because PB2 redundantly uses some sub-carriers that have no symbol energy. As a result effective noise power increases.

These simulations provide insights about the features of a state-of-the-art equalizer.

The performance comparison of equalizers under different channel conditions: The simulation results with the previously described algorithms are shown in Figures 2.6-2.10.

- In Figures 2.7-2.9 we see that an error floor comprises in all equalizers. It was being expected for the banded structures, because the neglected components of the spread energy increase the noise level at all SNR's. It was not expected for *MMSE* equalizer. It seems that the noise enhancement also increases with the mobility, because the non-banded serial equalizer given in [13] does not have an error floor.

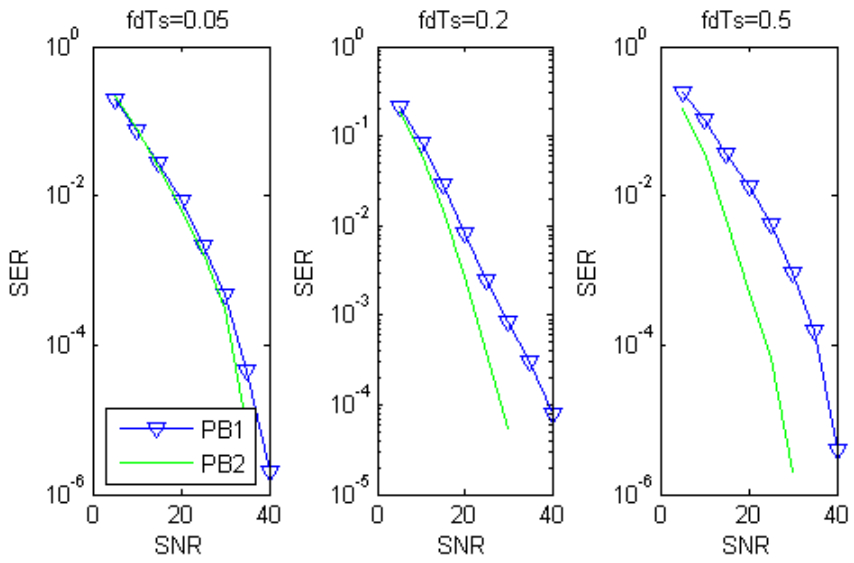

Figure 2.3: SER vs SNR for *PB1* and *PB2* with 4QAM under ITU Mod. Veh. A Channel

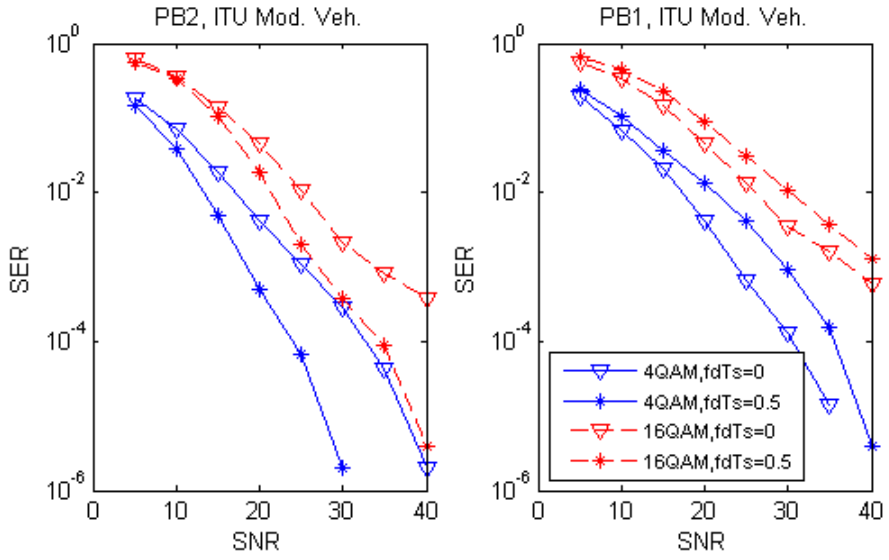

Figure 2.4: SER vs SNR for *PB1* and *PB2*

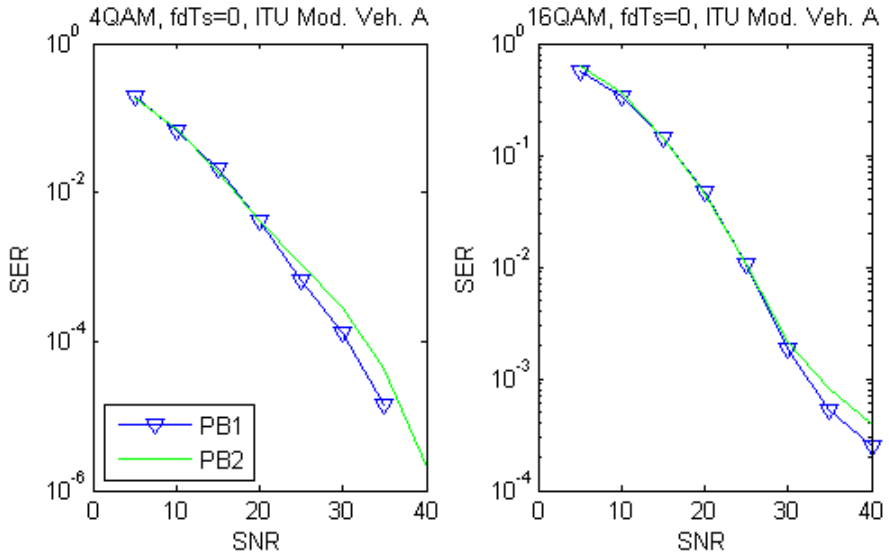

Figure 2.5: SER vs SNR for *PB1* and *PB2*

- Unlike *PB2*, the frequency diversity adversely affected the performances. In serial equalizers, wrong symbol estimates increase the interference power as the mobility increases. Block equalizers have the noise enhancement problem which grows with the mobility as stated above.

- Serial equalizers outperformed the block equalizers. This shows that the noise enhancement problem of block equalizers is more destructive than the increase of interference power resulting from wrong symbol estimates in serial equalizers.

- Compare the serial equalizer *TI* and the block equalizer *MMSE* with 4QAM and 16QAM modulations. *TI* is better with 4QAM while MMSE is as good as *TI* with 16 QAM. The reason is that the serial equalizers use the symbol estimates to remove ICI and the probability of wrong decision increases at the higher order modulations.

- The importance of ICI removal is clearly seen from the Figure 2.10. Even *TI*, which has the best performance, cannot perform as well as *PB1* which uses only the main diagonal of the channel matrix.

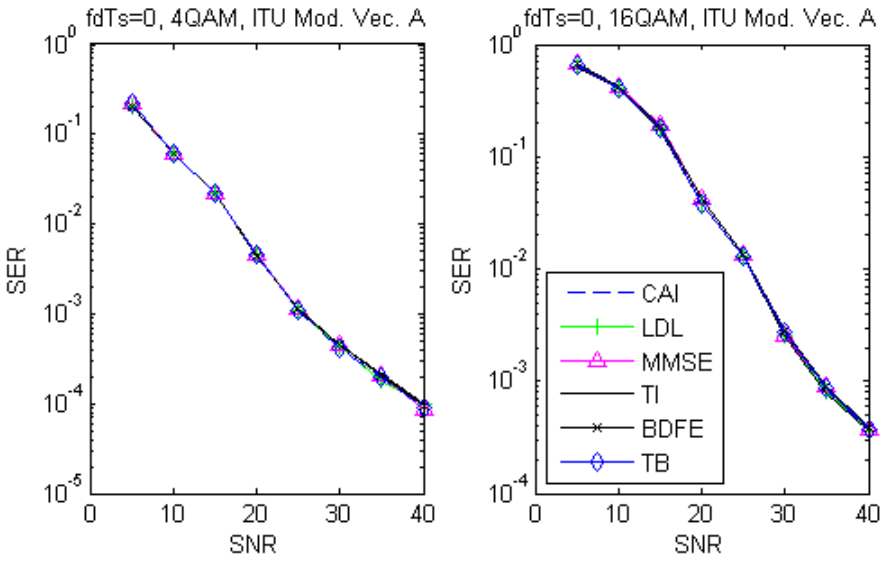

Figure 2.6: SER vs SNR for implemented algorithms for v=0km/h

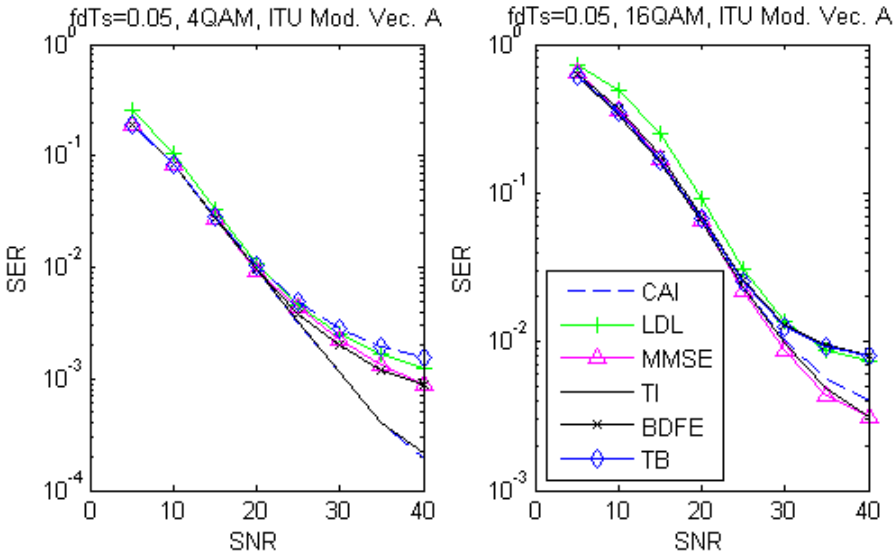

Figure 2.7: SER vs SNR for implemented algorithms for v=236km/h

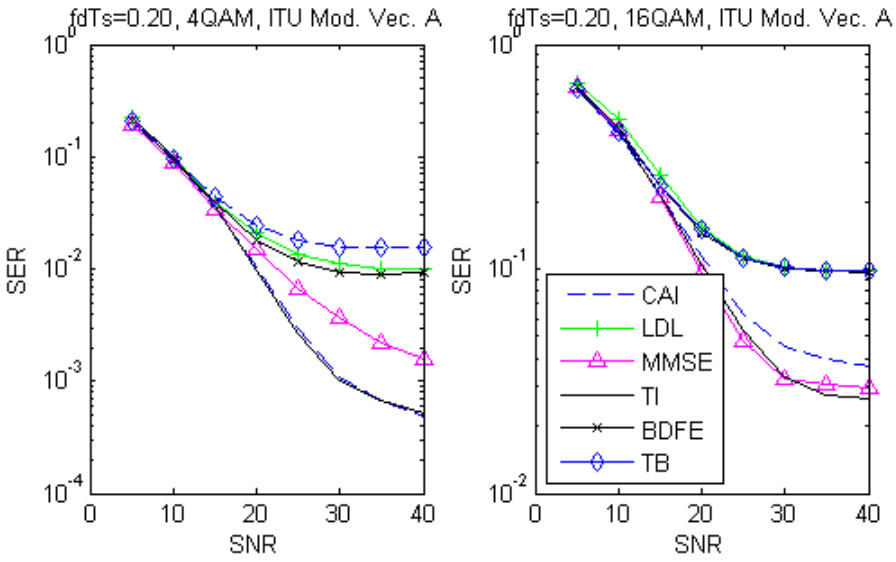

Figure 2.8: SER vs SNR for implemented algorithms for v=944km/h

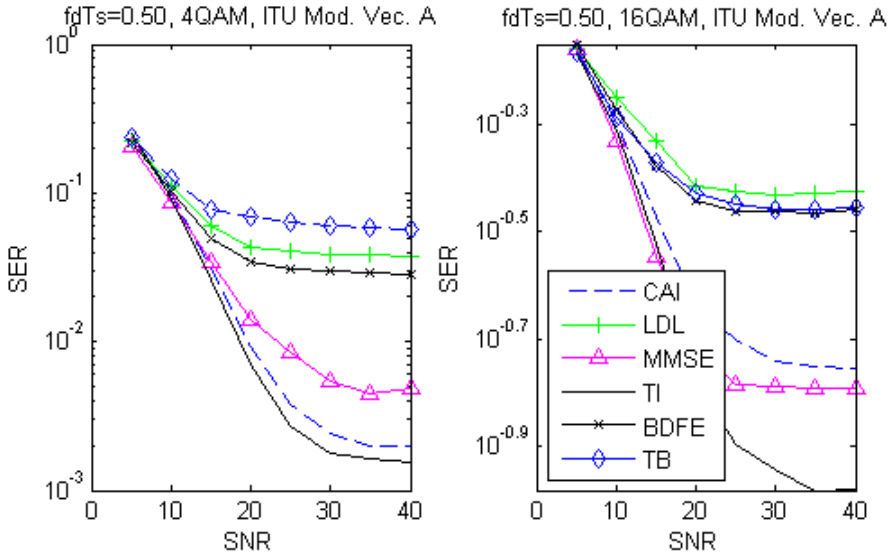

Figure 2.9: SER vs SNR for implemented algorithms for v=2360km/h

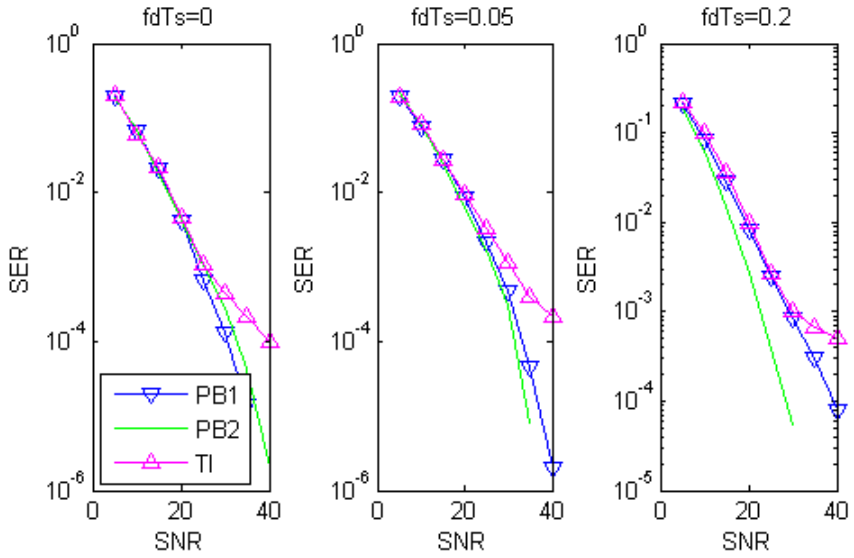

Figure 2.10: SER vs SNR for *TI*, *PB1* and *PB2* with 4QAM under ITU Mod. Veh. Channel

The effect of performance enhancement methods: First, *PIC* will be given. Because of its high complexity, *PIC* is not investigated in detail. Only one simulation is done which is given in Figure 2.11.

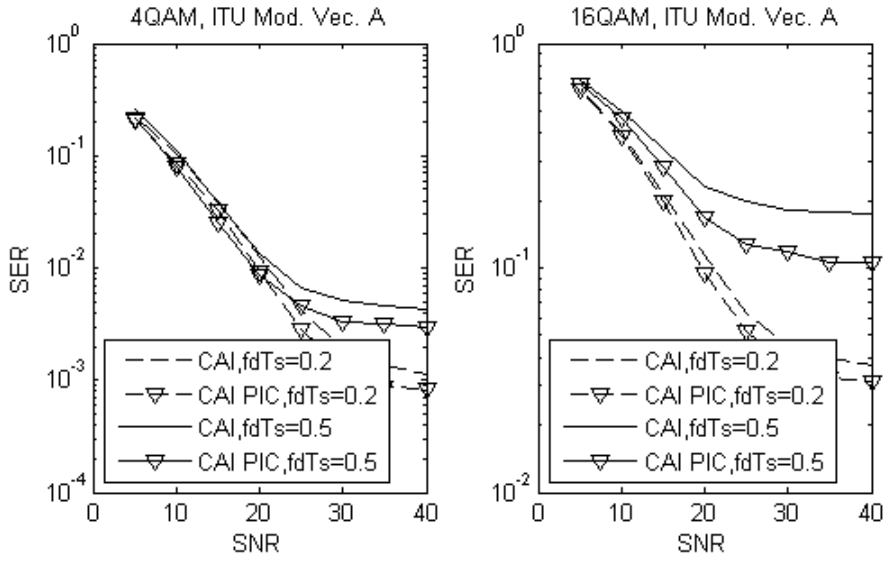

Figure 2.11: SER vs SNR with parallel interference calculation after *CAI*

The aim of windowing is to squeeze the spread energy into a few sub-carriers. This is shown in Figure 2.12. In the figure, the lines at the first index are the

average powers of main diagonal of the channel matrix, the next ones are the powers of the first super-diagonals and so on.

In Figure 2.13 the effect of windowing on *LDL*'s performance is simulated. As it is seen windowing provides a good performance improvement for *LDL*. In Figure 2.14, the effect of windowing on *TI*'s performance is shown. Unlike *LDL*, the performance degraded. This implies that interference power enhancement due to wrong symbol estimates dominate the gain coming from the ICI squeezing.

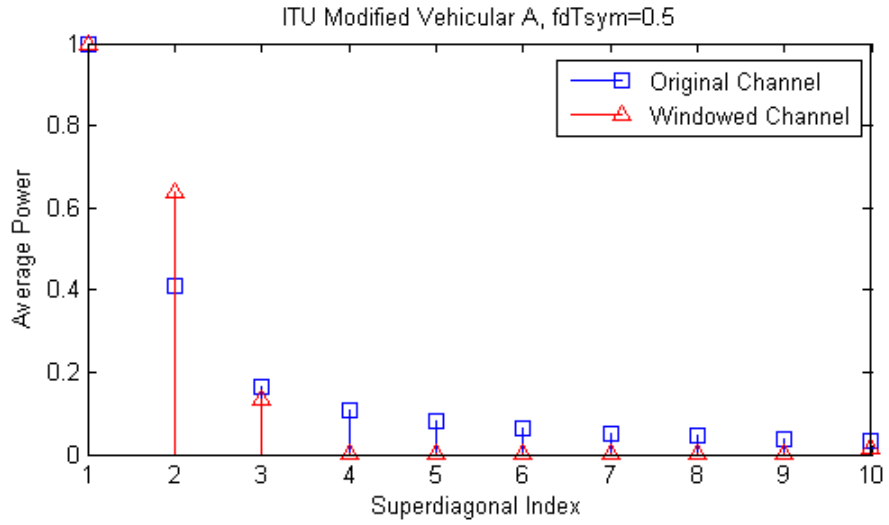

Figure 2.12: Average power of the main diagonal and the next 9 super diagonals

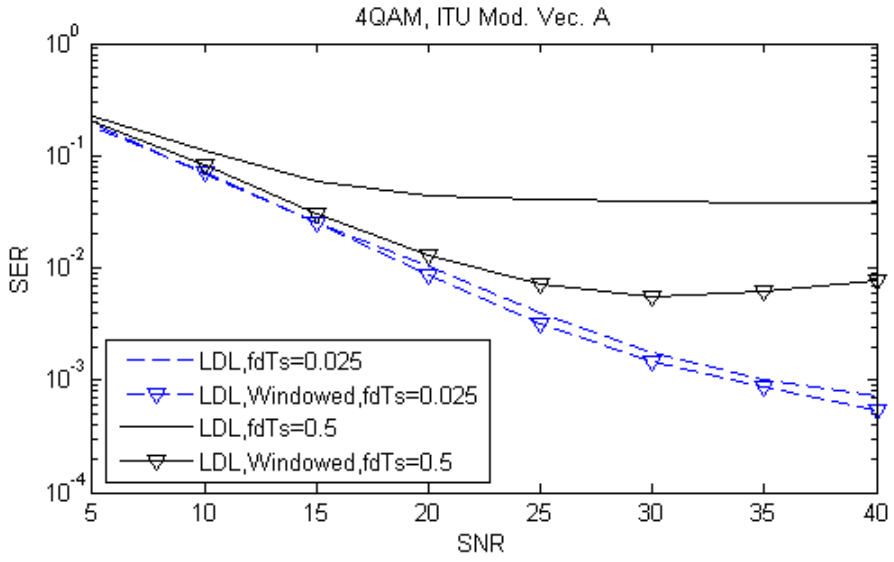

Figure 2.13: SER vs SNR with windowing of *LDL*

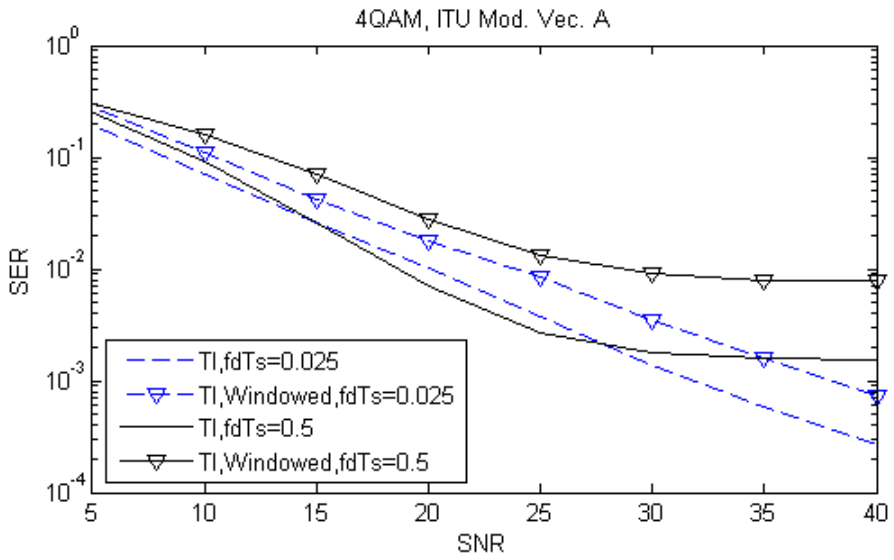

Figure 2.14: SER vs SNR with windowing of *TI*

Complexity comparison of some of the simulated equalizers: We will compare the complexities of the algorithms in terms of complex multiplications (CM) and divisions (CD) since they are the most costly operations in hardware. CD is even more difficult than CM, because there are no dedicated circuits that can perform division. The number of CD dominates the overall complexity because of that reason.

The complexity equations are given in Table 2.3 and in Figure 2.15 with respect to Q and normalized with the number of sub-carriers. The complexity equations of the first two rows are taken from [20] and [19] and modified for reduced number of CD. To calculate the complexity of *TB* again the same equations are used. The complexity of *TI* is calculated by assuming the inversion involved in *TI* is done according to method given in [22]. Neglecting the initial inversion, $20Q^2 + 10Q + 2$ CM and 2 CD per sub-carrier are required for the inversion, $8Q^2 + 6Q + 1$ CM per sub-carrier are required for the rest of the method.

Equalizer	No of CM	No of CD	Extras
BDFE	$4Q^2 + 14Q + 2$	2	noise power estimation
LDL	$4Q^2 + 14Q + 2$	2	noise power estimation
TI	$28Q^2 + 16Q + 3$	2	noise power estimation
TB	$8Q^2 + 16Q + 5$	4	square rooting + noise power estimation
MF	$4Q^2 + 6 + 2$	1	None
MMSE	More than N^2		noise power estimation
LS	More than N^2		None
CAI	More than N		noise power estimation

Table 2.3: Complexity equations of algorithms

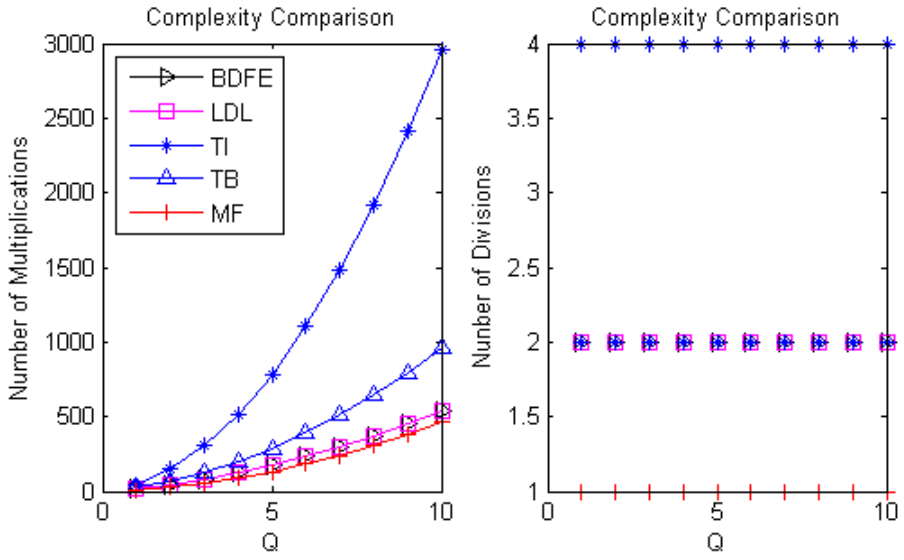

Figure 2.15: The normalized complexity comparison of some algorithms

2.4 Chapter Summary

At first a simulation was done with *PB1* and *PB2* to show the importance of using the power on the neighboring sub-carriers. *PB2* outperformed *PB1*, because *PB2* uses more energy than *PB1*. It is also shown by a simulation that the ICI creates a natural frequency diversity as the mobility increases. For that reason *PB2* performs better at high mobilities.

The serial equalizers *TI* and *CAI* outperformed the block equalizers. Also even the non-banded *MMSE* has an error floor at high mobilities, but the non-banded serial equalizer given in [13] does not. These results show that the noise enhancement problem of block equalizers is more destructive than the increase of interference power resulting from wrong symbol estimates in serial equalizers. Windowing provides an improvement for the block equalizers, however the result is still not as good as serial equalizers. The serial equalizers do not benefit from windowing, because interference power enhancement due to wrong symbol estimates dominates the gain coming from the ICI squeezing. Another drawback of serial ICI cancellation is that the interference power will grow with the modulation order, because the number of wrong symbol estimates will increase. This fact is corrected by comparing the performances of *MMSE* and *TI* with 4QAM and 16 QAM.

To show the importance of ICI cancellation, a simulation is done with *PB1*, *PB2* and *TI*. It is observed that even *TI* cannot perform as well as *PB1*, which uses only the main diagonal of the channel matrix. The error floor at high SNR values also prove this. For the banded equalizers, the unremoved/unused ICI energy create a noise floor, which becomes effective at high SNRs.

Based on the simulations and the discussion above we can say that a good equalizer should

- use the spread energy on the neighboring sub-carriers
- employ serial equalization
- employ a state-of-the-art ICI cancellation method

In terms of complexity the best one is *MF*. However its mobility range is very limited. At the mobilities where the performance of *MF* is not enough, *LDL* can

be used since it has the second lowest complexity and does not require iterations. After a limit TI is the only choice because of its performance and complexity.

Chapter 3

Proposed Modifications

Existing equalizers were presented in the second chapter. Based on the performance and complexity results, there was no state-of-the-art solution. In this chapter two modifications will be proposed. It will be shown by simulations that one of them is the closest one to a state-of-the-art solution within certain mobilities. The other modification will be proposed to *TI*, which was the best equalizer among the existing low complexity solutions in terms of performance. The proposed modification will decrease the complexity without any performance degradation.

3.1 Description of Proposed Modifications

The names of the modified algorithms are given below.

- Modified parallel interference cancellation (in short MPIC)
- Modified serial turbo equalization (in short MTI)

MPIC: This is a modified version of the parallel interference cancellation method given in Eq.(2.22). Equalization is performed serially. After going through all sub-carriers, a new iteration is started. At the beginning the sub-carrier which has the best SNR is found by ordering the absolute value of the diagonal of channel matrix. Equalization process is started from that sub-carrier and then moved forward or backward. Assume K^{th} sub-carrier has the best SNR. The next steps for the i^{th} iteration are summarized in Figure 3.1(MATLAB notation used).

for k =mod$(K + (0 : N - 1), N)$
  $\mathbf{p}_1$ =mod$([k - Q \ \ldots \ k + Q], N)$
  $\mathbf{p}_2$ =mod$([k - 4Q \ \ldots \ k + 4Q], N)$
  $\mathbf{a}_k = A(\mathbf{p}_1, k)$
  %equalization step
  $\mathbf{Y}(\mathbf{p}_2) = \mathbf{Y}(\mathbf{p}_2) + \hat{\mathbf{s}}(k)A(\mathbf{p}_2, k)$
  $\tilde{\mathbf{s}}(k) = (\mathbf{a}_k^H \mathbf{Y}(\mathbf{p}_1))/(\mathbf{a}_k^H \mathbf{a}_k)$
  %ici cancellation
  $\hat{\mathbf{s}}(k)$ =Slicer$(\tilde{\mathbf{s}}(k))$
  $\mathbf{Y}(\mathbf{p}_2) = \mathbf{Y}(\mathbf{p}_2) - \hat{\mathbf{s}}(k)A(\mathbf{p}_2, k)$
end

Figure 3.1: The pseudo code for *MPIC*

Before the first iteration $\hat{\mathbf{s}}$ is initialized to $\mathbf{0}_N$. Four iterations were done in the simulations.

MTI: This is a modified version of serial turbo equalization method *TI*. In TI algorithm, equalization and ICI cancellation is done by one equation given which is given in (2.15). We separated these two and used the same method in *MPIC*. The process for the i^{th} iteration is given in Figure 3.2 (MATLAB notation used). 3 iterations were done in the simulations. The complexity gain comes from the ICI removing mechanism. In *TI*, redundant multiplications are done to remove ICI for each sub-carrier.

The scenarios that will be simulated in the next section are described below:

for k =mod$(K + (0 : N - 1), N)$
$\mathbf{p}_1$ =mod$([k - Q \ \ldots \ k + Q], N)$
$\mathbf{p}_2$ =mod$([k - 2Q \ \ldots \ k + 2Q], N)$
$\mathbf{a}_k = \mathbf{A}(\mathbf{p}_1, k)$
$\mathbf{A}_k = \mathbf{A}(\mathbf{p}_1, \mathbf{p}_2)$
%equalization step
$\mathbf{Y}(\mathbf{p}_2) = \mathbf{Y}(\mathbf{p}_2) + \hat{\mathbf{s}}(k)\mathbf{A}(\mathbf{p}_2, k)$
$\mathbf{f}_k = (\mathbf{A}_k\mathbf{A}_k^H + \sigma^2 I_{2Q+1})^{-1}\mathbf{a}_k$
$\tilde{\mathbf{s}}k = \mathbf{f}_k^H\mathbf{Y}(\mathbf{p}_1)$
%ici cancellation
$\hat{\mathbf{s}}(k)$ =Slicer$(\tilde{\mathbf{s}}(k))$
$\mathbf{Y}(\mathbf{p}_2) = \mathbf{Y}(\mathbf{p}_2) - \hat{\mathbf{s}}(k)A(\mathbf{p}_2, k)$
end

Figure 3.2: The pseudo code for *MTI*

- The performance comparison of *TI*, *MPIC*, *MTI* and *PB2*.
- The performances of *TI*, *MPIC* and *MTI* with different parameters.
- Complexity comparison of algorithms

3.2 Simulations and Comments

The primary objective of the simulations in this section is to suggest an equalization method for use in current systems.

The performance comparison of equalizers: In Figures 3.3-3.6 the performances of *TI*, *MPIC*, *MTI* and *PB2* are compared. Until 120km/h they perform close to each other (The mobility at 120km/h meets the mobility requirements of WiMAX). After that speed, *MPIC* falls behind the others. The remaining two, *TI* and *MTI*, are better than *MPIC* at high mobilities. *MPIC* ignores ICI in the first iteration, that is why it has a bad performance at high mobilities.

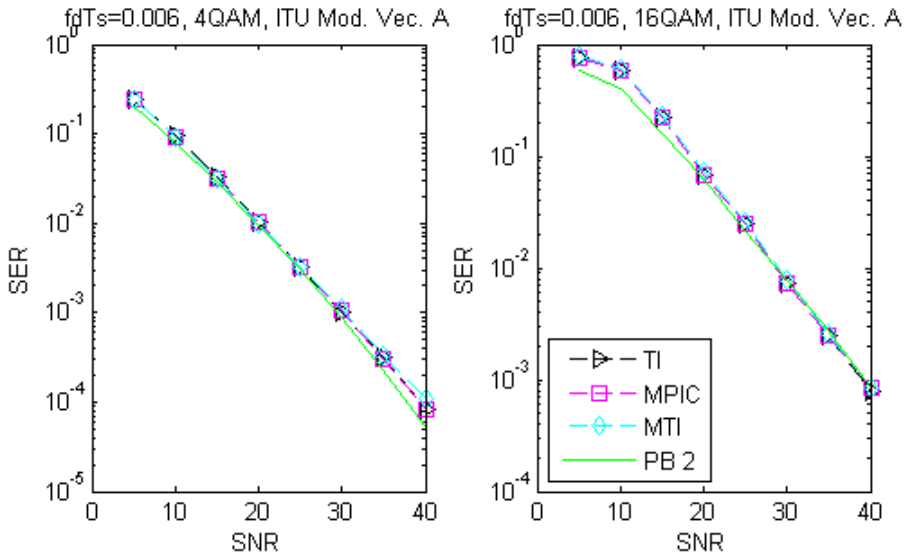

Figure 3.3: SER vs SNR for v=30km/h

The performances of selected and proposed algorithms with different parameters: In Figures 3.7-3.9 the performances of *TI*, *MPIC* and *MTI* are shown separately. The individual effects of some parameters on the equalizer performances are investigated. The *normal* stands for the default parameters. For example the default parameters of *TI* are: $Q = 2$, 3 iterations and no windowing.

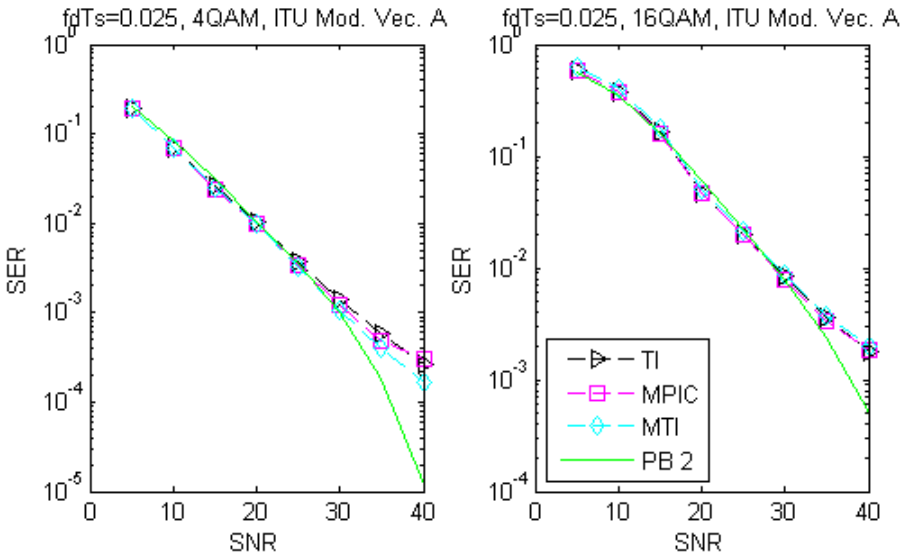

Figure 3.4: SER vs SNR for v=120km/h

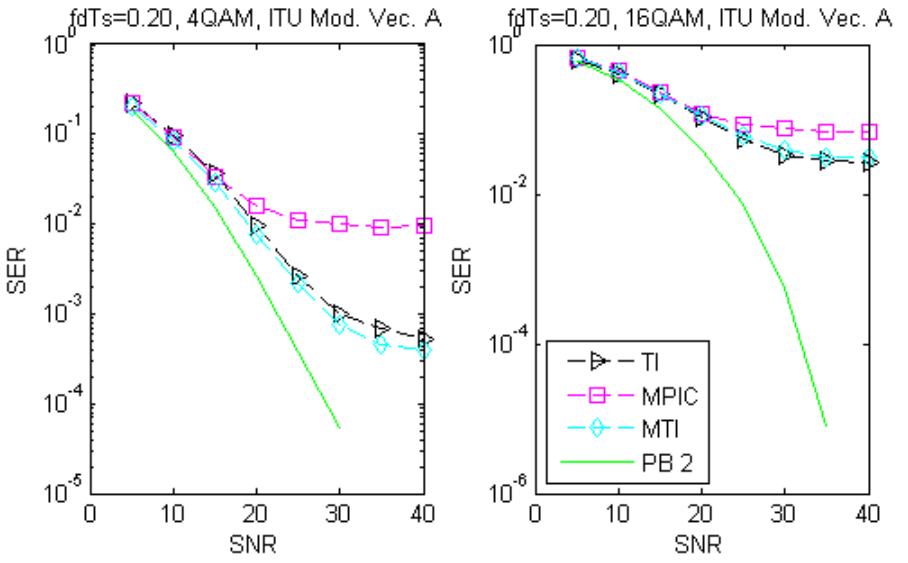

Figure 3.5: SER vs SNR for v=944km/h

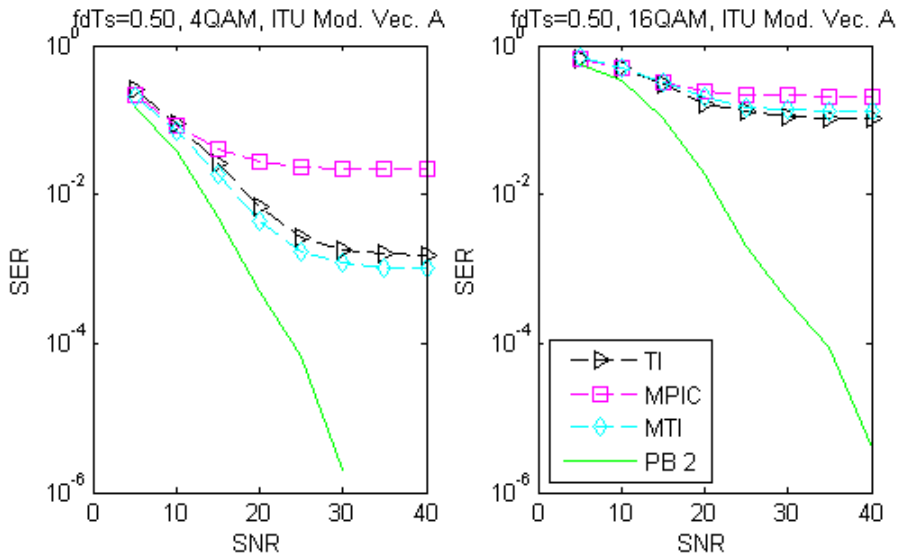

Figure 3.6: SER vs SNR for v=2360km/h

In chapter two, it was seen that windowing degraded the performance of *TI*. The same degradation occurred for *MTI* and *MPIC*. The explanation of the degradation for *TI* was given in the second chapter which is valid for *MTI*. For *MPIC* the reason is a bit different. In the first iteration *MPIC* assumes that there is no ICI. However the ICI power increases within the band of interest after windowing. Neglecting this power terribly effects performance.

Fortunately the number of iterations does not enhance the performance of any of the three. However the increase of band-width of the equalizers does. More energy is used for equalization and more ICI cancellation is done, so the performance increase is normal.

Complexity comparison of algorithms: As in the previous chapter the complexities will be given in terms of complex multiplications and divisions. The complexity of *MPIC* is obvious. While calculating the complexity of *MTI*, we assumed that the inversion operation is done according to the procedure given in [22] which requires $20Q^2 + 10Q + 2$ CM and 2 CD per sub-carrier. For the rest of the method only $4Q + 1$ CM per sub-carrier are needed.

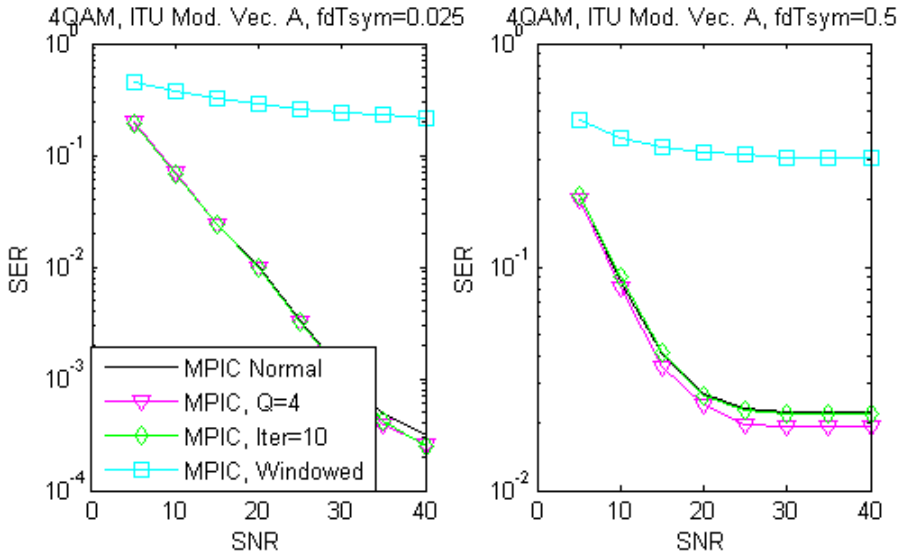

Figure 3.7: The effect of some parameters on *MPIC* equalizer

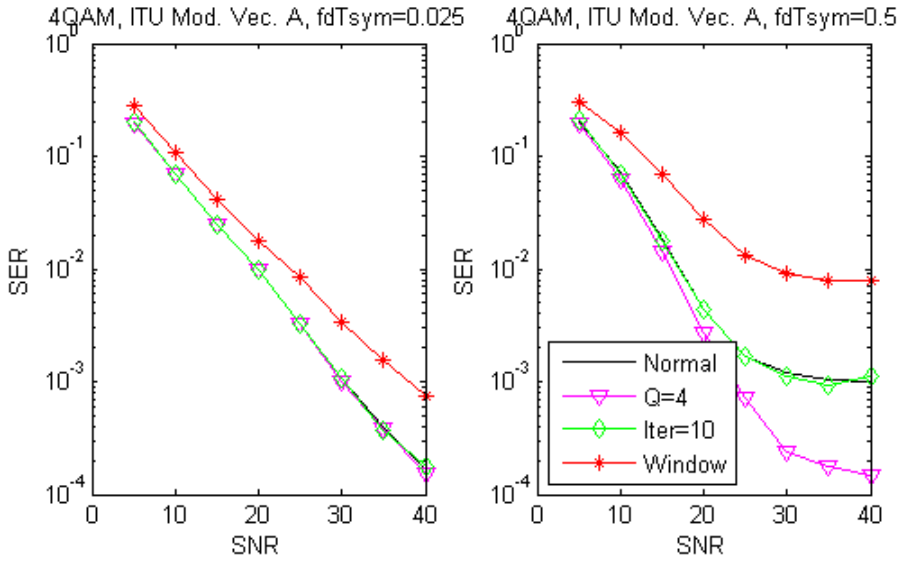

Figure 3.8: The effect of some parameters on *MTI* equalizer

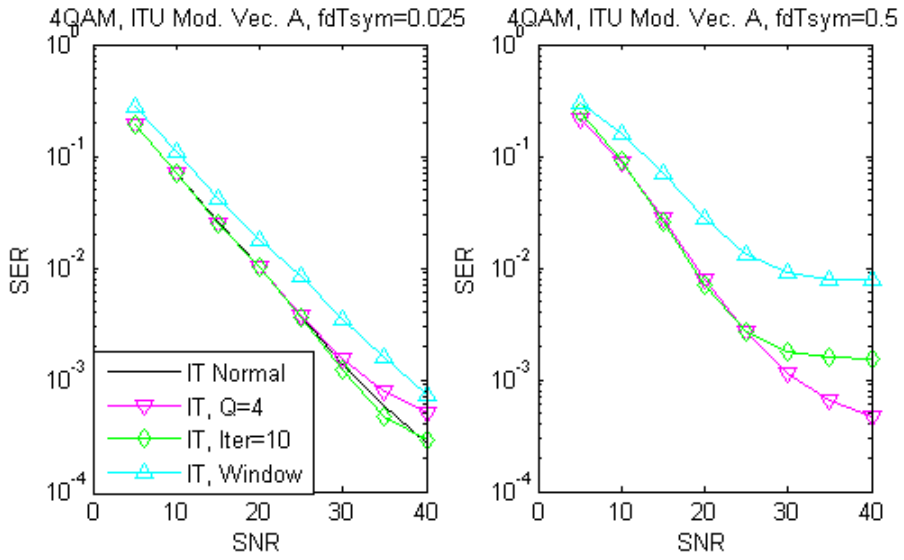

Figure 3.9: The effect of some parameters on *TI* equalizer

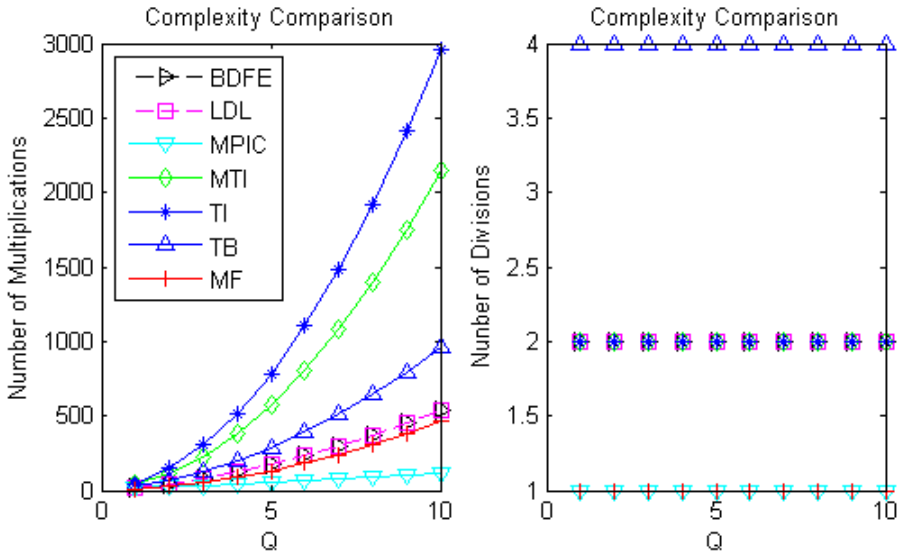

Figure 3.10: The normalized complexity comparison of some algorithms

Equalizer	No of CM	No of CD	Extras
BDFE	$4Q^2 + 14Q + 2$	2	noise power estimation
LDL	$4Q^2 + 14Q + 2$	2	noise power estimation
TI	$28Q^2 + 16Q + 3$	2	noise power estimation
TB	$8Q^2 + 16Q + 5$	4	square root + noise pow. est.
MF	$4Q^2 + 6 + 2$	1	None
MMSE	More than N^2		noise power estimation
LS	More than N^2		None
CAI	More than N		noise power estimation
MPIC	$11Q + 3$	1	None
MTI	$20Q^2 + 14Q + 3$	2	noise power estimation

Table 3.1: Complexity equations of algorithms

3.3 Chapter Summary

The primary objective of this chapter was to present a state-of-the-art equalizer. Up to speeds of 120km/h, at which the mobility meets the requirements of WiMAX, *MPIC* method is the closest of all to a state-of-the-art solution. The complexity of *MPIC* is at least 2 times better than the least complex algorithm (neglecting *MF*). However its performance is not good at high mobilities, because in the first iteration *MPIC* ignores the ICI. On the other hand the increase of bandwidth assumption of the channel matrix enhances the performance, because the energy, that is used for equalization, and the ICI power, that is removed from the observation vector, also increases.

The modification to *MTI* reduced the complexity of *TI* at least 25 percent without any performance degradation. Even though the complexity of *MTI* is still higher than the other low complexity methods. The increase of bandwidth assumption of the channel matrix improves the performance as with *MPIC*. Fortunately the number of iterations does not provide any enhancement.

Finally, based on the performances and complexities we suggest the following algorithms

- *MF* at low mobilities
- *MPIC* where *MF* starts to fail
- *MTI* where *MPIC* starts to fail

Chapter 4

Summary and Future Work

The objectives of this thesis were given in the first chapter as

- to investigate the effects of time variation of the channel on OFDM
- to present the existing solutions
- to propose new solutions
- to provide intuition for further developments

The discussions about these objectives will be given in the following paragraphs.

The intercarrier interference, which is a result of time variation of the channel, was introduced in the first chapter. In the second chapter, some simulations were done about the effects of ICI on an OFDM system. Basically ICI is the loss of the orthogonality of the subcarriers within an OFDM symbol. In other words the channel matrix that is given in Eq.(1.11) becomes a non-diagonal matrix. The energy of the main diagonal spreads over the neigboring super-diagonals and sub-diagonals. Intuitively all the spread energy should be used for a good performance. The simulation that was given in Figure 2.3 proved that intuition. Also it was stated that the energy spreading could be viewed as

a natural frequency diversity which improves the performance. The simulation that was given in Figure 2.4 proved that it was true. On the other hand it was observed by the simulations of the existing equalization algorithms that frequency diversity did not work when all the sub-carriers were modulated, because the ICI components could not be removed perfectly.

The existing solutions proposed in the literature were presented and simulated in the second chapter. The primary objective of implementing many equalizers was to find a state-of-the-art algorithm. The state-of-the-art definition according to this thesis was given in the first chapter. A state-of-the-art solution should have

- the performance of *PB2*.
- a complexity less than $N \log N$ which is the complexity of FFT algorithm.

In terms of complexity only the *MF* equalizer was a state-of-the-art method, whose mobility was very limited. In terms of performance the best ones were *TI*, *CAI* and *MMSE*, but again they could not perform as well as *PB2* after some mobilities. The complexities of *CAI* and *MMSE* were too high and the complexity of *TI* was the largest one among the remaining ones. In other words there was no state-of-the-art solution in the literature.

In the third chapter the proposed modifications were presented. Some of the algorithms given in the second chapter were close to a state-of-the-art solution. However the *MPIC*, which was obtained by modifying *PIC*, became the closest of all in terms of complexity. *MPIC*'s complexity was at least two times better than the least complex algorithm (neglecting *MF*). Also the noise power estimation was not required, while the other candidates did. On the other hand the mobility range was again limited. After some mobilities *MPIC* fell behind the *PB2*. Fortunately this mobility limit met the mobility requirements of WiMAX. The second modification was proposed to *TI*. As explained above, in terms of

performance it was the best candidate at high mobilities for a state-of-the-art solution. Its complexity was reduced by at least 25 percent and the performance remained the same with the proposed modification. Nevertheless the resulting complexity was still the largest one among the remaining low complexity solutions. In conclusion the state-of-the-art could not be achieved, but still there were low complexity solutions which were realizable. Based on the performance and complexity results given in the second and third chapter, the following algorithms were suggested for use in current systems:

- *MF* at low mobilities
- *MPIC* where *MF* starts to fail (bandwidth of the equalizer can be increased for better performance)
- *MTI* where *MPIC* starts to fail (bandwidth of the equalizer can be increased for better performance)

The final objective was to provide guidelines for a state-of-the-art solution. From simulations of *PB1* and *PB2* in the second chapter it was deduced that the spread energy should be used. This result was also corrected by the simulations in the third chapter, because the increase of bandwidth assumption of the channel matrix improved the performances of *TI*, *MTI* and *MPIC*. A second property was obtained from the simulations of the existing equalizers. It was observed that serial equalizers outperformed block equalizers ([13]). This implied that the noise enhancement problem of block equalizers was more destructive than the increase of interference power resulting from wrong symbol estimates in serial equalizers. Thirdly, even if serial equalization was much better, there was another problem for serial ICI cancellation. Since the estimates were used, at higher order modulations the ICI cancellation would become worse because of the increase of the number of wrong decisions. The comparison of the performances of *TI* and *MMSE* with 4QAM and 16QAM verified this claim. Finally the performances of

TI, *PB1* and *PB2* were compared. *PB1*, which does not use the spread energy, outperformed *TI* at high mobilities even though *TI* uses the spread energy. The imperfect ICI cancellation was the cause of that. It was concluded that a state-of-the-art ICI cancellation should be found. *Windowing* was offered for that reason, however it enhanced only the performance of block equalizers, because the interference power enhancement of serial equalizers due to increase of the number of wrong symbol estimates dominated the gain coming from the ICI squeezing.

Based on the discussions above it can be said that a state-of-the-art equalizer should

- use the spread energy on the neighboring sub-carriers
- perform serial equalization
- cancel ICI
- use a state-of-the-art ICI cancellation, the existing methods have drawbacks

We think that there is no need to search for new equalizers. The major problem is ICI cancellation. As seen in *PB1* example, even the energy on the main diagonal is enough for good performances at high mobilities. Unless a state-of-the-art ICI cancellation is found, using OFDM at high mobilities is impossible with SISO configuration. For that reason one of our future work will be about the state-of-the-art ICI cancellation. Even though diversity methods are used, a state-of-the-art ICI cancellation will increase the performance further. Two techniques can be given here as an example. In [25] a self cancellation method is proposed while reducing the data rate by half. In [26] pulse shaping is employed at the transmitter at a cost of complexity.

Another important problem is channel estimation. In fact finding a low complexity channel estimation is a more difficult problem. Also the performance of

the channel estimator and equalizer will rely on each other. In the future work the equalizer structures given in this thesis will be tested with a channel estimator. Then a jointly state-of-the-art channel estimator and equalizer will be investigated based on the results.

Bibliography

[1] Cyril-Daniel Iskander, "A MATLAB-based Object Oriented Approach to Multipath Fading Channel Simulation," tech. rep., Hi-Tek Multisystems, 2008.

[2] P. A. Bello, "Characterization of Randomly Time Variant Linear Channels," *IEEE Trans. Comm.*, vol. COM-11, pp. 360–393, 1963.

[3] G. L. Turin, "A Statistical Model of Urban Multipath Propagation," *IEEE Trans. Veh. Tech.*, vol. VT-21, pp. 1–9, 1972.

[4] W. C. Jakes, *Microwave Mobile Communications*. New Tork: WILEY, 1974.

[5] Yunxin Li and Xiaojing Huang, "The Simulation of Independent Rayleigh Faders," *IEEE Trans. Comm.*, vol. 9, pp. 1503–1514, 2002.

[6] R. W. Chang, "Synthesis of Bandlimited Orthogonal Signals For Multichannel Data Transmission," *Bell System Tech. Jour.*, pp. 1775–1796, 1966.

[7] S. B. Weinstein and P. M. Ebert, "Data Transmission by Frequency Division Multiplexing Using Discrete Fourier Transform," *IEEE Trans. Comm.*, vol. 19, pp. 628–634, 1971.

[8] W. Zou and W. Yiyan, "COFDM: An overview," *IEEE Trans. Broadcast*, vol. 41, pp. 1–8, 1995.

[9] G. B. Giannakis, "Filterbanks For Blind Channel Identification and Equalization," *IEEE Signal Proc.*, vol. 4, pp. 184–187, 1997.

[10] M. Weiss, "WIMAX: General Information About the Standard 802.16," tech. rep., Rohde and Schwarz, 2006.

[11] ANSI T1E1.4 Committee Contribution, *The DWMT: A Multicarrier Transciever For ADSL Using M-band Wavelets*. 1993.

[12] R. van Nee and R. Prasad, *OFDM For Wireless Multimedia Communications*. Artech House Publishers, 2000.

[13] Y. S. Choi, P. J. Voltz and F. A. Cassara, "On Channel Estimation and Detection for Multicarrier Signals in Fast and Selective Rayleigh Fading Channels," *IEEE Trans. Comm.*, vol. 49, pp. 1–13, 2001.

[14] P. Schniter, "Low Complexity Equalization of OFDM in Doubly Selective Channels," *IEEE Trans. Signal Proc.*, vol. 52, pp. 1002–1011, 2004.

[15] Ramjee Prasad, *OFDM for Wireless Communications Systems*. Artech House, 2004.

[16] Ahmad R. S. Bahai, Burton R. Saltzberg, Mustafa Ergen, *Multi-Carrier Digital Communications*. Springer, 2004.

[17] Henrik Schulze and Christian Luders, *Theory and Applications of OFDM and CDMA*. Wiley, 2005.

[18] "IEEE 802.16m Evaluation Methodology Document (EMD)," 2009. IEEE 802.16m-08/004r5.

[19] L. Rugini, P. Banelli and G. Leus, "Simple Equalization of Time-Varying Channels for OFDM," *IEEE Trans. Comm.*, vol. 9, pp. 619–621, 2005.

[20] L. Rugini, P. Banelli and G. Leus, "Low Complexity Banded Equalizers for OFDM Systems in Doppler Spread Channels," *Eurasip Jour. on Applied Signal Proc.*, vol. 2006, pp. 1–13, 2006.

[21] Kun Fang and Geert Leus, "Low-Complexity Block Turbo Equalization For OFDM Systems In Time- and Frequency-Selective Channels," *The Third Annual IEEE BENELUX/DSP Valley Signal Processing Symposium*, pp. 83–87, 2007.

[22] X. Cai and G. B. Giannakis, "Bounding Performance and Suppressing Intercarrier Interference in Wireless Mobile OFDM," *IEEE Trans. Comm.*, vol. 51, pp. 2047–2056, 2003.

[23] L. L. Scharf, *Statistical Signal Processing: Detection, Estimation, and Time Series Analysis*. Addison Wesley, 1991.

[24] N. Al-Dhahir and A. H. Sayed, "The Finite-Length Multi-Input Multi-Output MMSE-DFE," *IEEE Trans. Signal Proc.*, vol. 48, pp. 2921–2936, 2000.

[25] Y. Zhao and S. Häggman, "Intercarrier Interference Self-Cancellation Scheme For OFDM Mobile Communication Systems," *IEEE Trans. Comm.*, vol. 49, pp. 1185–1191, 2001.

[26] Volkan Kumbasar and Oguz Kucur, "ICI Reduction In OFDM Systems by Using Improved Sinc Power Pulse," *Digital Signal Processing*, vol. 17, pp. 997–1006, 2007.